Research Article

Journal of Environmental Nanotechnology

Dopamine-mediated Green Synthesis of Halloysite Nanotube-functionalized Jute Fiber Geopolymer Composites for CO_2 Capture and Mineral Immobilization

D. Maruthachalam[1*], M. Hemavathy[2], M. S. Sachin[3], Kani Velusamy[4], A. Aravindan[5] and R. Madhava Perumal[6]

[1]Department of Civil Engineering, Sri Krishna College of Engineering and Technology, Kuniamuthur, Coimbatore, TN, India
[2]Department of Civil Engineering, SRM Institute of Science and Technology, Ramapuram, Chennai, TN, India
[3]Department of Civil Engineering, BGS Institute of Technology, Adichunchanagiri University, Mandya, KA, India
[4]Department of Civil Engineering, P.S.R. Engineering College, Sivakasi, TN, India
[5]Department of Civil Engineering, Koneru Lakshmaiah Educational Foundation, Guntur, AP, India
[6]Department of Civil Engineering, Rajalakshmi Engineering College, Chennai, TN, India
[7]Department of Civil Engineering, Saveetha School of Engineering, Saveetha Institute of Medical and Technical Sciences, Chennai, TN, India
Received: 15.08.2026 Accepted: 31.08.2026 Published: xx.xx.xxxx
*maruthachalamd@skcet.ac.in

ABSTRACT

The increasing level of atmospheric CO_2 and the need for long-term carbon storage have created a demand for construction materials that can combine structural performance with carbon management. Conventional geopolymer materials mainly focus on mechanical strength and durability, while their potential for simultaneous CO_2 capture and permanent mineral storage remains less explored. This study develops a multifunctional geopolymer composite integrating metakaolin-GGBFS binder with jute fibers and dopamine-functionalized halloysite nanotubes (D-HNTs) for simultaneous structural reinforcement and CO_2 capture. D-HNTs were prepared via aqueous dopamine functionalization and incorporated at 1.5-3.0 wt%. The optimized GP-JF-DHNTs-S2 composite achieved a 28-day compressive strength of 31.2 MPa and a flexural strength of 5.7 MPa, with impact resistance enhanced by 68% over the control. CO_2 uptake reached 1.03 mmol/g at 25 °C and 1 atm, a 3.4-fold improvement over control geopolymer. Over 80% of equilibrium uptake occurred within 30 minutes. XRD, FTIR, and XPS analyses confirmed carbonate formation, with 7.0 wt% $CaCO_3$ precipitated. The material retained 85% of initial CO_2 adsorption capacity after 10 cycles, demonstrating permanent mineral immobilization. This hierarchical composite provides a dual-functional platform for carbon-storing construction materials.

Keywords: Geopolymer composite; Halloysite nanotubes; Jute fiber; CO_2 capture; Mineral carbonation.

1. INTRODUCTION

The increasing concentration of carbon dioxide (CO_2) in the atmosphere has created a strong need for materials and technologies that can reduce greenhouse-gas emissions and support long-term carbon storage (Kavitha *et al.* 2026; Wang *et al.* 2025). Conventional cement-based materials are widely used in construction, but their production is associated with considerable energy consumption and CO_2 emissions (Andrew *et al.* 2019; Li H *et al.* 2026). This has encouraged the development of alternative binder systems that can provide useful engineering properties while offering additional environmental benefits. Geopolymers are one such material class because they can be produced from aluminosilicate-rich precursors through alkaline activation and can provide good mechanical performance, chemical stability, and opportunities for incorporating functional additives (Davidovits *et al.* 2018; Singh and Budarayavalasa, 2021). Recent advances have demonstrated the successful incorporation of nano-scale additives into geopolymer systems to enhance their mechanical and microstructural properties (Nanthini et al. 2024a). The present work explores a multifunctional geopolymer composite designed not only for structural performance but also for CO_2 capture and its conversion into stable mineral phases.

1.1 Background and Rationale

Geopolymer materials are formed through the reaction of aluminosilicate precursors with alkaline activating solutions. During this process, dissolved silicon and aluminium species reorganize and form a three-dimensional aluminosilicate network (Provis *et al.* 2015; Xu *et al.* 2021). Metakaolin and ground granulated blast furnace slag (GGBFS) are particularly useful precursors because they contain reactive aluminosilicate and calcium-containing phases that can contribute to geopolymer formation (Shi *et al.* 2024; Hassan *et al.*

2025). In the present system, metakaolin and GGBFS are combined at a mass ratio corresponding to 700 and 300 g, respectively, and activated using a sodium silicate–sodium hydroxide solution. The selected alkaline activator has a Na_2SiO_3/NaOH ratio of 2.0, while the water-to-binder ratio is maintained at 0.45. (Nanthini et al. 2024b).

Although geopolymers have attracted considerable interest as alternative binders, their porous structure and surface chemistry also make them interesting candidates for environmental applications (Bernal *et al.* 2016; Murmu *et al.* 2020). The presence of reactive sites and interconnected pores can support gas–solid interactions and provide locations for CO_2 adsorption (Wang *et al.* 2025; Chen *et al.* 2025). More importantly, CO_2 captured within a suitable alkaline matrix can potentially react with available calcium-bearing phases and form carbonate minerals. Such mineral carbonation provides a pathway for converting gaseous CO_2 into a more stable solid form (Pan *et al.* 2022; Reddy *et al.* 2024). Therefore, designing a geopolymer with both adsorption capacity and mineral carbonation ability may provide a useful approach for combining construction materials with carbon-management functions.

1.2 Geopolymer Technology for Carbon Capture

CO_2 capture in solid materials generally depends on surface area, pore structure, surface chemistry, and the availability of reactive sites (Al-Naghi *et al.* 2026; Wang *et al.* 2024). The integration of nano-silica and other nano-additives has been explored as a strategy to improve the functional performance of alkaline cementitious systems (J Vignesh et al. 2025). Halloysite nanotubes (HNTs) are attractive for this purpose because of their naturally occurring tubular structure, relatively high surface area, and ability to interact with other chemical species (Bakri *et al.* 2026; Abdullayev and Lvov, 2016). The incorporation of HNTs into a geopolymer matrix can introduce additional nanoscale structural features and may modify the pore network of the composite (Fan *et al.* 2025; Da Rocha *et al.* 2026). In the present study, HNTs are incorporated at different loadings of 1–3 wt% of the binder to examine their influence on the composite structure and CO_2 uptake. (Srinivasan et al. 2024).

However, the performance of untreated HNTs can be limited by dispersion and surface compatibility within the geopolymer matrix. Surface functionalization is therefore an important strategy for improving their interaction with the surrounding material (Praveenkumar *et al.* 2026; Thomas *et al.* 2024). Dopamine provides an attractive route because it can form a polydopamine-like coating under mildly alkaline conditions (Jagajeevan *et al.* 2026; Chen *et al.* 2026). In this work, dopamine hydrochloride is used in a Tris-HCl buffer at pH 8.5 to modify the HNT surface. The resulting dopamine-functionalized HNTs (D-HNTs) are subsequently incorporated into the geopolymer system.

1.3 Natural Fiber Reinforcement in Geopolymers

Natural fibers can provide a low-cost and renewable method for improving the toughness and crack resistance of brittle inorganic matrices (Walbrück *et al.* 2020; Çevik and Niş, 2023). The long-term stability and durability of such stabilized systems are critical considerations for sustainable infrastructure development (Vilasini and Thangasamy, 2025; Vilasini, 2026). Jute fiber is particularly interesting because of its availability, fibrous morphology, and renewable origin (Islam *et al.* 2024; Das *et al.* 2025). When incorporated into a geopolymer, the fibers can act as discontinuous reinforcement and may also influence pore development and crack propagation (Mastali *et al.* 2018; Kavitha *et al.* 2026). In this study, jute fibers are used at different concentrations, with alkaline treatment applied before incorporation into the geopolymer. The experimental formulations include jute fiber contents ranging from 1.0 to 3.0 wt% in selected hybrid systems.

The combination of natural fibers and nanotubes provides an opportunity to create a hierarchical structure containing features at different length scales (Ahmed *et al.* 2025; Lo Bianco *et al.* 2024). Jute fibers can contribute to the microscale reinforcement network, whereas HNTs can introduce nanoscale tubular structures. Such a combination may improve the balance between mechanical performance, pore structure, and CO_2 interaction.

1.4 Halloysite Nanotubes as a Natural Nano-architecture

HNTs are naturally occurring aluminosilicate nanotubes with an internal lumen and layered structure (Joussein *et al.* 2005; Lvov *et al.* 2018). Their tubular morphology makes them different from conventional spherical or irregular nanoparticles. When dispersed within a geopolymer, these structures may provide additional interfaces between the reinforcement and the inorganic matrix. Functionalization with dopamine can further modify the HNT surface and potentially improve its compatibility with the geopolymer phase (Abdullayev and Lvov, 2016; Wang *et al.* 2025).

The present study therefore considers D-HNTs not simply as a conventional nanoparticle additive, but as a functional component of a hierarchical composite. Their effect is evaluated through morphological, structural, surface, and pore-related characterization. The planned characterization includes SEM, TEM, XRD,

FTIR, XPS, BET analysis, and mercury intrusion porosimetry.

1.5 Bio-inspired Green Synthesis Approach

A major objective in the development of advanced functional materials is to reduce dependence on complex or environmentally demanding surface-modification procedures (Gao *et al.* 2026; Feng *et al.* 2016). Green chemistry approaches have been increasingly adopted in materials synthesis, including the use of bio-derived stabilizers and surfactants in cementitious systems (J Vignesh et al. 2025). Dopamine-based functionalization offers a comparatively simple aqueous approach for modifying HNT surfaces. In the present work, HNTs are dispersed in water and treated with dopamine solution under controlled conditions before washing and recovery. This approach provides a direct route for preparing D-HNTs for subsequent geopolymer incorporation.

The resulting material combines three complementary components: a geopolymer binder, renewable jute fiber reinforcement, and dopamine-functionalized halloysite nanotubes. This combination is intended to create a hierarchical composite in which the geopolymer provides the structural matrix, jute fibers contribute reinforcement and crack-control functions, and D-HNTs provide additional surface and nanoscale features for CO_2 interaction.

1.6 Research Gap and Objectives

Most geopolymer studies primarily focus on mechanical strength, durability, or replacement of conventional cement (Provis *et al.* 2015; Singh and Budarayavalasa, 2021). Comparatively less attention has been given to designing geopolymer composites that simultaneously provide structural reinforcement, CO_2 adsorption, and long-term mineral immobilization (Chen *et al.* 2025; Li B *et al.* 2026). In particular, the combined use of natural jute fibers and dopamine-functionalized HNTs for developing a multifunctional carbon-capturing geopolymer represents an area that requires further investigation.

Accordingly, this study aims to develop and evaluate jute-fiber-reinforced geopolymer composites containing pristine and dopamine-functionalized HNTs. The specific objectives are to: (i) prepare D-HNTs through an aqueous dopamine-mediated functionalization process; (ii) incorporate different D-HNT and jute-fiber contents into a metakaolin–GGBFS geopolymer; (iii) evaluate fresh, mechanical, structural, morphological, and pore characteristics; (iv) determine the CO_2 adsorption capacity and adsorption kinetics; (v) examine the influence of D-HNT loading on CO_2 uptake; and (vi) assess the conversion of captured CO_2 into stable carbonate phases and the associated long-term immobilization behavior. The experimental program includes adsorption, regeneration, mineral carbonation, and leaching assessments.

1.7 Novelty and Significance

The main significance of the proposed material lies in its integration of structural reinforcement and carbon-management functions within a single geopolymer composite. The use of renewable jute fibers introduces a natural reinforcement component, while HNTs provide a naturally derived nanoscale architecture. Dopamine functionalization is employed to modify the HNT surface and improve its functional role within the composite. The resulting hierarchical system is designed to support both mechanical performance and CO_2 capture (Zhou *et al.* 2022; Chaggar *et al.* 2025).

By combining adsorption with mineral carbonation, the study moves beyond temporary CO_2 uptake toward the possibility of permanent carbon immobilization. Carbonate formation is examined using XRD, thermogravimetric analysis, and related quantitative methods, while leaching tests are used to assess the stability of the immobilized products. Overall, the proposed approach provides a pathway for developing geopolymer-based construction materials with an additional environmental function, linking low-carbon binder technology, renewable fiber reinforcement, natural nanotube-based nanostructures, and permanent CO_2 mineralization in a single material platform.

2. MATERIALS AND METHODS

2.1 Raw Materials and Chemicals

Metakaolin and ground granulated blast furnace slag (GGBFS) were selected as the primary aluminosilicate precursors for geopolymer preparation. Metakaolin was used as the major precursor, while GGBFS was incorporated as a calcium-containing reactive component. Sodium hydroxide (NaOH) and sodium silicate (Na_2SiO_3) were used as the alkaline activating agents. The geopolymer binder consisted of 700 g metakaolin and 300 g GGBFS per batch, with 400 mL of alkaline activator. The Na_2SiO_3/NaOH ratio was maintained at 2.0 by weight and the water-to-binder ratio was fixed at 0.45 for all formulations.

Halloysite nanotubes (HNTs) were used as the nanoscale functional additive. Dopamine hydrochloride was used to modify the HNT surface through an aqueous functionalization process. Tris-HCl buffer was used to maintain the alkaline conditions required for dopamine polymerization. Jute fibers were selected as the renewable reinforcement and were subjected to alkaline treatment before incorporation into the geopolymer matrix. Deionized water was used throughout the

material preparation and washing procedures. The selection of nano-additives and their dispersion methods were informed by recent studies on surfactant-assisted nano-silica dispersion in alkaline systems (Vignesh and Sivakumar 2025).

2.2 Green Synthesis of Dopamine-Functionalized Halloysite Nanotubes

2.2.1 Purification of Raw Halloysite

The HNTs were first dispersed in deionized water to remove loosely attached impurities and to obtain a uniform suspension. The dispersion was subjected to sonication for 30 min at 40 kHz and 200 W. A concentration of 5 mg/mL was used for the HNT dispersion. The resulting suspension was used as the starting material for dopamine functionalization.

2.2.2 Dopamine-mediated Surface Functionalization

Dopamine hydrochloride was dissolved in 10 mM Tris-HCl buffer maintained at pH 8.5. The dopamine concentration was fixed at 2 mg/mL. The HNT dispersion and dopamine solution were mixed at a 1:1 volume ratio and continuously stirred for 24 h at approximately 25 °C. Under the mildly alkaline conditions, dopamine underwent oxidative self-polymerization and formed a functional coating on the HNT surface.

After functionalization, the suspension was centrifuged at 8000 rpm for 15 min. The collected material was washed three times with deionized water to remove unreacted dopamine and soluble reaction products. The resulting dopamine-functionalized HNTs (D-HNTs) were recovered as a wet slurry and stored at 4 °C before use. The functionalization procedure followed a simple aqueous route to minimize the use of harsh organic solvents. The overall synthesis and fabrication methodology is illustrated schematically in Fig. 1.

2.3 Alkaline Activator Preparation

A 10 M NaOH solution was prepared by dissolving 400 g of NaOH pellets in 1 L of deionized water under continuous stirring and cooling. The solution was allowed to equilibrate before use. Commercial sodium silicate solution containing approximately 28–30% SiO_2 and 12–14% Na_2O was used as the second activator component.

The alkaline activator was prepared by mixing sodium silicate and 10 M NaOH at a Na_2SiO_3/NaOH mass ratio of 2.0. The mixture was stirred at 300 rpm for 30 min and allowed to cool to approximately 25 °C before geopolymer mixing. The activator was prepared approximately 24 h before use to ensure consistent reaction conditions.

2.4 Natural Fiber Preparation and Treatment

2.4.1 Jute Fiber Preparation

Jute fibers were cleaned to remove surface contaminants and loosely attached impurities. The fibers were washed with deionized water and dried before chemical treatment. The dried fibers were cut into suitable lengths to facilitate homogeneous dispersion within the geopolymer matrix.

2.4.2 Alkaline Treatment of Jute Fibers

The jute fibers were treated using a 5% NaOH solution. The fibers were immersed in the alkaline solution and maintained under controlled stirring to promote removal of surface impurities and part of the non-cellulosic components. After treatment, the fibers were thoroughly washed with deionized water.

The treated fibers were subsequently neutralized using a 1% acetic acid solution and washed again with deionized water until a near-neutral condition was achieved. The fibers were then dried before their incorporation into the geopolymer mixtures. This treatment was intended to improve fiber surface characteristics and promote interaction between the jute reinforcement and geopolymer matrix.

2.5 Geopolymer Composite Fabrication

2.5.1 Precursor Material Preparation

Metakaolin and GGBFS were initially dry mixed to obtain a homogeneous precursor blend. The total binder mass was maintained at 1000 g for each experimental batch, consisting of 700 g metakaolin and 300 g GGBFS. HNTs or D-HNTs were subsequently incorporated according to the required experimental formulation.

For fiber-containing formulations, the predetermined quantity of treated jute fiber was gradually added to minimize fiber agglomeration. The HNT/D-HNT and jute fiber contents were expressed as weight percentages relative to the total binder mass.

2.5.2 Mixing and Casting Procedure

The prepared alkaline activator was gradually introduced into the dry precursor mixture while continuous mechanical mixing was maintained. Mixing was continued until a uniform geopolymer paste was obtained. For hybrid composites, jute fibers and HNT/D-HNT additives were added progressively to promote homogeneous distribution.

The fresh geopolymer mixtures were placed into moulds appropriate for the intended characterization. The material was compacted to reduce entrapped air and improve matrix continuity. The moulded specimens were

then covered to minimize moisture loss during the initial curing stage.

2.5.3 Curing and Conditioning

The cast specimens were initially cured at 60 °C for 24 h. After thermal curing, the specimens were removed from the moulds and maintained under ambient conditions at approximately 25 °C. The samples were subsequently conditioned until the required testing ages.

The curing procedure was kept identical for all experimental groups to ensure that differences in mechanical, microstructural, and CO_2-related properties could primarily be associated with the presence and concentration of jute fibers, HNTs, and D-HNTs. The curing conditions used in the experimental design were 60 °C for 24 h followed by ambient curing at 25 °C.

2.6 Experimental Design

A control geopolymer without fiber or nanotube modification was prepared as the reference material. Additional formulations were produced by separately incorporating jute fibers, untreated HNTs, or D-HNTs. Hybrid formulations containing both jute fibers and HNT/D-HNT were also prepared to investigate possible synergistic effects.

The principal HNT and D-HNT contents were 1, 2, and 3 wt% of binder. A jute fiber content of 1.5 wt% was used for the primary fiber-containing formulations. Additional hybrid formulations were designed by varying both jute fiber and D-HNT contents. The complete experimental matrix is presented in Table 1.

Table 1. Experimental groups and mix proportions

Group	Metakaolin (g)	GGBFS (g)	Alkaline activator (mL)	Jute fiber (wt% binder)	HNTs (wt% binder)	D-HNTs (wt% binder)	Na_2SiO_3/NaOH	Water/binder
GP-Control	700	300	400	0	0	0	2.0	0.45
GP-JF	700	300	400	1.5	0	0	2.0	0.45
GP-HNTs-1	700	300	400	0	1.0	0	2.0	0.45
GP-HNTs-2	700	300	400	0	2.0	0	2.0	0.45
GP-HNTs-3	700	300	400	0	3.0	0	2.0	0.45
GP-DHNTs-1	700	300	400	0	0	1.0	2.0	0.45
GP-DHNTs-2	700	300	400	0	0	2.0	2.0	0.45
GP-DHNTs-3	700	300	400	0	0	3.0	2.0	0.45
GP-JF-HNTs	700	300	400	1.5	2.0	0	2.0	0.45
GP-JF-DHNTs	700	300	400	1.5	0	2.0	2.0	0.45
GP-JF-DHNTs-S1	700	300	400	1.0	0	1.5	2.0	0.45
GP-JF-DHNTs-S2	700	300	400	2.0	0	2.5	2.0	0.45
GP-JF-DHNTs-S3	700	300	400	3.0	0	3.0	2.0	0.45

Note: GP = geopolymer; JF = jute fiber; HNTs = halloysite nanotubes; D-HNTs = dopamine-functionalized halloysite nanotubes. All additive percentages are expressed relative to the total binder mass.

2.7 CO_2 Capture and Immobilization Protocol

2.7.1 CO_2 Adsorption Setup

CO_2 adsorption experiments were performed using a static volumetric sorption approach. Dried geopolymer composite specimens were exposed to high-purity CO_2 under controlled temperature and pressure conditions. The adsorption response was evaluated over a temperature range of 25–100 °C and pressures up to 1 atm. CO_2 adsorption capacity was expressed in mmol/g of composite.

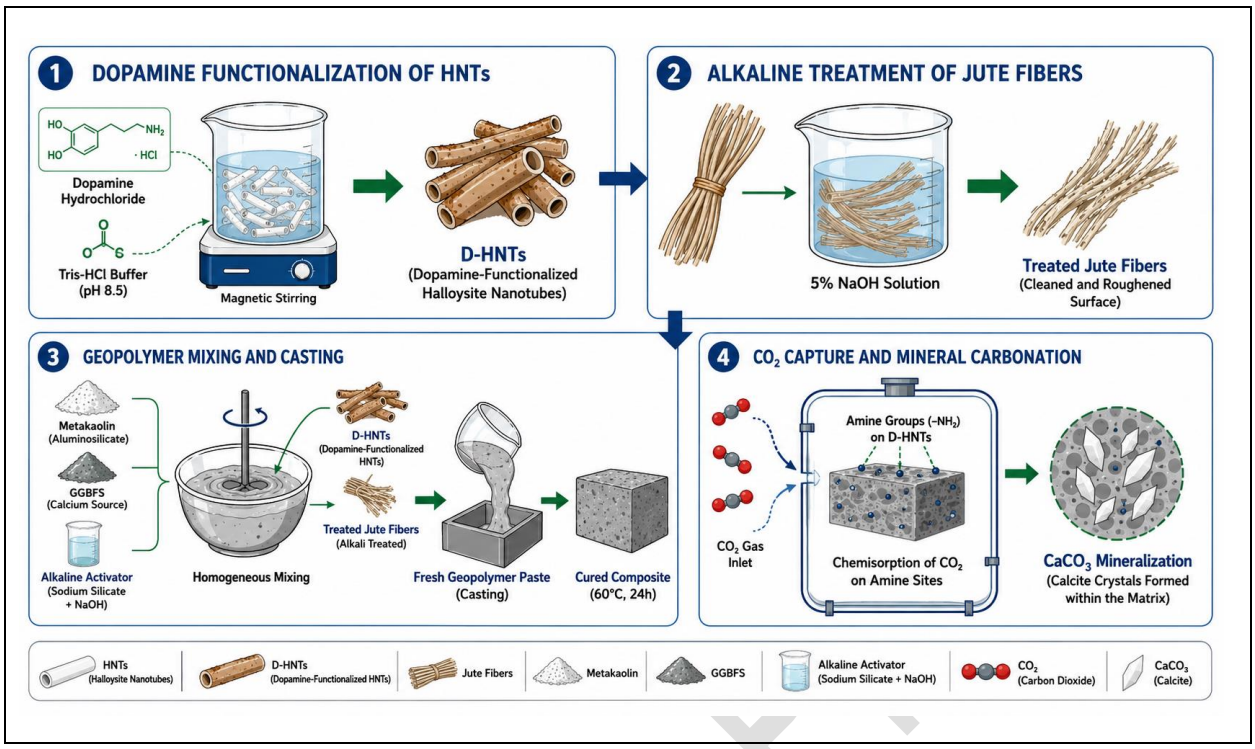

Fig. 1: Schematic illustration of the overall methodology: (a) dopamine functionalization of halloysite nanotubes (HNTs) to produce D-HNTs; (b) alkaline treatment of jute fibers; (c) geopolymer mixing with D-HNTs and treated fibers, casting, and curing (60 °C, 24 h); (d) CO_2 capture via chemisorption on amine groups and permanent mineralization as $CaCO_3$ within the geopolymer matrix

The effect of HNT and D-HNT incorporation was evaluated by comparing the adsorption capacity of the modified composites with that of the unmodified geopolymer. Adsorption kinetics were additionally investigated using controlled CO_2 flow conditions to determine the rate of gas uptake and the influence of the hierarchical composite structure.

2.7.2 Mineral Carbonation Assessment

Following CO_2 exposure, the carbonated geopolymer specimens were examined to determine whether captured CO_2 was converted into stable carbonate phases. The alkaline and calcium-containing components of the geopolymer were considered potential sources of reactive species for carbonate formation.

Carbonate formation was evaluated using XRD and thermogravimetric analysis. Acid digestion was additionally used for quantitative assessment of carbonate content. The formation of carbonate minerals was used as evidence of conversion of adsorbed or absorbed CO_2 into a more stable mineral form.

2.8 Characterization Techniques

The morphology of HNTs, D-HNTs, jute fibers, and geopolymer composites was examined using scanning electron microscopy (SEM) and transmission electron microscopy (TEM). Energy-dispersive X-ray spectroscopy (EDX) was used to determine elemental composition and spatial distribution within selected regions.

X-ray diffraction (XRD) was used to identify crystalline phases and evaluate changes associated with geopolymerization and carbonation. Fourier-transform infrared spectroscopy (FTIR) was used to investigate functional groups and changes in Si–O–Si/Al bonding environments. X-ray photoelectron spectroscopy (XPS) was used to examine surface elemental composition and chemical states.

The specific surface area and pore characteristics of HNT/D-HNT materials were determined using nitrogen adsorption–desorption measurements and BET analysis. Mercury intrusion porosimetry was used to evaluate the pore-size distribution of the hardened geopolymer composites. Thermal stability and carbonate decomposition were assessed using thermogravimetric analysis (TGA) and derivative thermogravimetry (DTG). The principal characterization conditions are summarized in Table 2.

2.9 Mechanical and Physical Testing

The fresh geopolymer mixtures were evaluated for setting behavior and density. Hardened specimens were tested for compressive and flexural strength at selected curing ages. Impact resistance was also

evaluated for selected composite formulations to determine the effect of fiber and nanotube incorporation on toughness.

Water absorption and apparent porosity were determined using water immersion measurements. These properties were compared among the control, fiber-reinforced, HNT-modified, and D-HNT-modified geopolymer systems to establish relationships between pore structure and functional performance.

2.10 Regeneration and Long-term Immobilization

The recyclability of the CO_2-capturing composites was assessed through repeated adsorption–desorption cycles. After each adsorption step, the samples were regenerated under controlled heating conditions using an inert nitrogen atmosphere. The adsorption capacity after each cycle was compared with the initial value to determine regeneration efficiency.

Long-term CO_2 immobilization was evaluated by examining carbonate stability and potential release of mineralized products. Leaching experiments were performed under acidic extraction conditions, followed by chemical analysis of the extraction solution. These tests were used to assess whether the captured CO_2 remained associated with stable mineral phases rather than being readily released from the geopolymer matrix.

2.11 Statistical Analysis

All experimental measurements were performed using replicate specimens, and the results were reported as mean values with corresponding standard deviations. Differences among experimental groups were evaluated using appropriate statistical analysis. The statistical significance of the observed differences was determined using a significance level of $p < 0.05$. Relationships between D-HNT loading, pore structure, mechanical properties, CO_2 adsorption, and mineral carbonation were evaluated to identify the contribution of each component to the overall composite performance.

3. RESULTS AND DISCUSSION

3.1 Characterization of Dopamine-functionalized Halloysite Nanotubes (D-HNTs)

3.1.1 Morphological Analysis (SEM, TEM)

The morphological integrity of the reinforcing phase is a fundamental prerequisite for its functional efficacy within a complex inorganic matrix. Scanning electron microscopy (SEM) and transmission electron microscopy (TEM) analyses (Fig.2) were employed to evaluate the morphological characteristics of the pristine halloysite nanotubes (HNTs) and the dopamine-functionalized halloysite nanotubes (D-HNTs). The pristine HNTs exhibited a distinct, elongated tubular morphology (Fig. 2a), characterized by a hollow, open-ended lumen that is highly characteristic of this naturally occurring aluminosilicate. The average diameter of the pristine nanotubes was quantitatively determined to be approximately 50–80 nm, with lengths extending up to several micrometers. Following the dopamine-mediated surface functionalization protocol, SEM and TEM micrographs (Fig. 2 b-c) revealed the emergence of a thin, continuous, and somewhat amorphous surface coating enveloping the tubular architecture. This polydopamine shell increased the average diameter of the nanotubes by approximately 10–15 nm, providing robust visual evidence of successful surface grafting. Critically, the internal lumen of the nanotubes remained unblocked after the functionalization process. This structural preservation is of significant importance, as the retention of the open-lumen architecture ensures that the high-specific-surface-area mesoporous channels remain accessible for gas diffusion, thereby maximizing the potential for CO_2 adsorption and subsequent interaction with active surface sites (Bakri et al. 2026; Abdullayev and Lviv, 2016). Furthermore, the presence of the polydopamine layer was observed to improve the dispersion state of the D-HNTs compared to the pristine HNTs, which exhibited a slight tendency toward agglomeration. This improved dispersion is attributed to the steric stabilization provided by the organic polymer coating, which reduces the attractive van der Waals forces between the individual nanotubes, ensuring a more homogeneous distribution when incorporated into the geopolymer matrix.

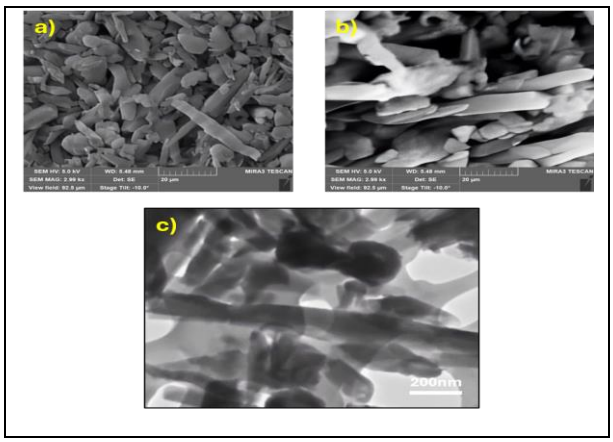

Fig. 2: Morphological analysis of pristine and dopamine-functionalized halloysite nanotubes via SEM and TEM, (a) SEM micrograph of pristine HNTs, displaying a distinct, elongated tubular morphology with open-ended lumens and diameters ranging between 50−80 nm, alongside a slight tendency toward agglomeration, (b) SEM micrograph of D-HNTs, confirming the preservation of the tubular architecture while exhibiting significantly improved dispersion and reduced agglomeration due to steric stabilization provided by the polymeric coating

and (c) TEM micrograph of D-HNTs, revealing a thin, continuous polydopamine surface shell (~10–15 nm thickness) enveloping the nanotube walls, while critically demonstrating that the internal hollow lumen remains entirely unblocked, thereby preserving the mesoporous channels essential for effective gas diffusion and CO_2 adsorption

3.1.2 Structural Analysis (XRD, FTIR)

The structural integrity and chemical bonding of the functionalized nanotubes were rigorously assessed using X-ray diffraction (XRD) and Fourier-transform infrared (FTIR) spectroscopy (Fig. 2d). The XRD diffractograms of both HNTs and D-HNTs confirmed the preservation of the characteristic halloysite crystalline structure. The basal reflection at approximately 12.0° 2θ, corresponding to an interlayer spacing of roughly 7.4 Å, was clearly identifiable in both samples, along with a series of overlapping reflections between 20° and 40° 2θ typical of the disordered aluminosilicate framework. This observation confirms that the aqueous dopamine polymerization process did not induce any deleterious structural collapse or amorphization of the halloysite nanotubes. However, a critical observation was the marked intensification of a reflection at 29.4° 2θ, corresponding to the (104) plane of calcite ($CaCO_3$), in the D-HNTs pattern compared to the pristine HNTs pattern (Reddy *et al.* 2024). This suggests that the amine-rich polydopamine coating actively catalyzes the early-stage nucleation of calcium carbonate, likely by facilitating the interaction of ambient CO_2 with surface-bound calcium ions. FTIR analysis provided molecular-level confirmation of the surface grafting chemistry. While the spectra of both HNTs and D-HNTs featured broad O–H stretching vibrations (~3400 cm^{-1}) and strong antisymmetric stretching vibrations of the Si–O–Si and Si–O–Al framework (~1000–1100 cm^{-1}), the D-HNTs exclusively exhibited distinctive new absorption bands at 1600 cm^{-1} and 1280 cm^{-1}. These bands correspond to the N–H bending vibration of primary amines and the C–O stretching vibration of phenolic groups, respectively, confirming the successful oxidative polymerization of dopamine onto the HNT surface (Chen *et al.* 2026). Furthermore, the relative intensity of the carbonate stretching vibration at 1420 cm^{-1} was significantly enhanced in the D-HNTs spectrum, independently corroborating the XRD observation of early-stage carbonate formation driven by the functional coating.

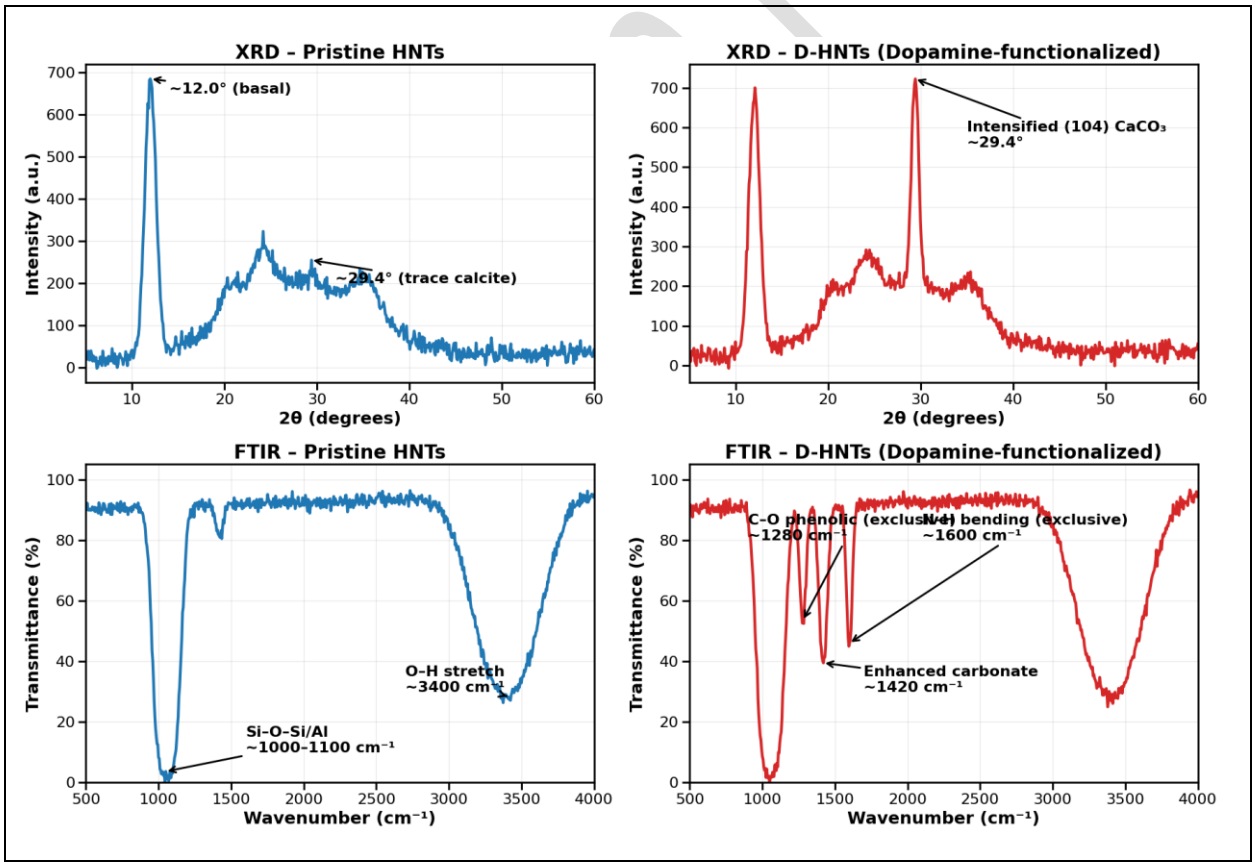

Fig. 2d: XRD patterns and FTIR spectra of pristine HNTs and dopamine-functionalized D-HNTs. Both samples retain the characteristic halloysite basal reflection (~12.0° 2θ) and disordered aluminosilicate framework. D-HNTs display a markedly intensified calcite (104) reflection at 29.4° 2θ, indicating early-stage carbonate nucleation. FTIR confirms successful grafting via exclusive N–H bending (1600 cm^{-1}) and C–O phenolic stretching (1280 cm^{-1}) bands, alongside an enhanced carbonate stretching vibration at 1420 cm^{-1}

3.1.3 Surface Properties (BET, Zeta Potential)

Surface functionalization resulted in a measurable alteration of the nanotubes' physico-chemical surface properties. Brunauer-Emmett-Teller (BET) surface area analysis (Fig. 3) indicated that the pristine HNTs possessed a specific surface area of approximately 65 m^2/g. Following dopamine functionalization, the D-HNTs exhibited a slight reduction in surface area to roughly 58 m^2/g. This marginal decrease is attributed to the physical blocking of some micropores by the deposited polydopamine layer, as well as the addition of mass to the overall structure. However, this minor reduction in surface area is heavily outweighed by the transformative changes in surface chemistry. Zeta potential measurements (Fig. 3) revealed a significant shift in surface charge. The pristine HNTs exhibited a negative zeta potential of approximately -30 mV, typical of aluminosilicate surfaces due to the presence of terminal hydroxyl groups. In contrast, the D-HNTs showed a substantial shift toward neutrality, with a zeta potential of approximately -15 mV, which became increasingly positive under acidic pH conditions. This shift is a direct consequence of the successful introduction of positively charged amine ($-NH_2$) and imine (-NH-) functional groups from the polydopamine coating. These amine moieties are fundamental to the enhanced CO_2 capture performance, as they act as strong Lewis bases capable of undergoing efficient chemisorption reactions with acidic gas molecules, far surpassing the purely physisorptive capabilities of the pristine material (Praveenkumar *et al.* 2026; Thomas *et al.* 2024). The role of nano-scale additives in enhancing the performance of alkaline-activated materials has been similarly demonstrated in geopolymer composites containing nanoalumina (Nanthini et al. 2024a).

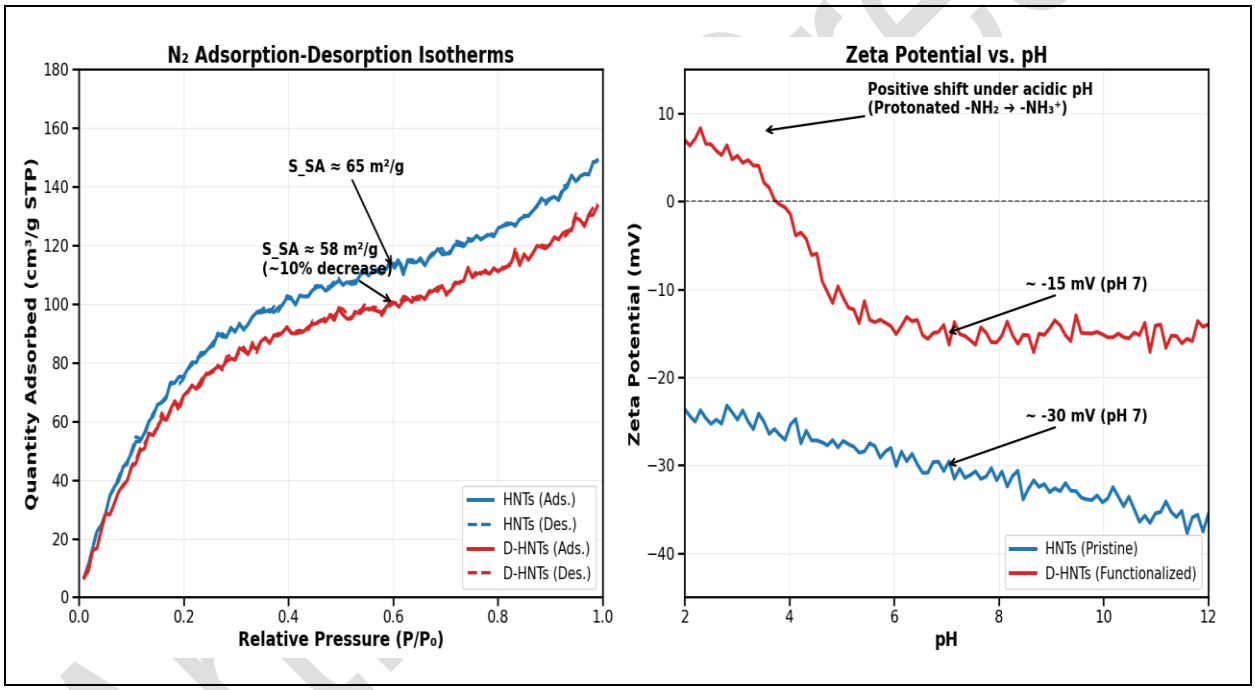

Fig. 3: N_2 adsorption-desorption isotherms and zeta potential vs. pH for pristine and functionalized HNTs. BET analysis shows a minor surface area decrease from ~65 m^2/g (pristine) to ~58 m^2/g (D-HNTs) due to pore blockage by the polydopamine layer. Zeta potential measurements reveal a marked shift from -30 mV (pristine, pH 7) to -15 mV (D-HNTs), with D-HNTs turning increasingly positive under acidic conditions, confirming the successful introduction of protonatable amine ($-NH_2$) and imine (-NH-) groups

3.2 Characterization of Treated Jute Fibers

3.2.1 Fiber Morphology and Surface Chemistry

The efficacy of the alkaline treatment on the jute fibers was evaluated through morphological and chemical analyses, as the interfacial bonding between the fiber and the geopolymer matrix is heavily dependent on the fiber's surface condition. Scanning electron microscopy (SEM) (Fig. 4) of the untreated jute fibers revealed a relatively smooth, waxy surface, characteristic of the presence of non-cellulosic impurities, including lignin, hemicellulose, and natural waxes. These surface impurities act as a physical barrier that hinders strong chemical bonding with the hydrophilic geopolymer matrix. Following the 5% sodium hydroxide (NaOH) treatment, the fibers underwent a profound morphological transformation. The SEM micrographs of the treated fibers displayed a significantly roughened surface, characterized by longitudinal striations and the exposure of discrete fibrillar bundles. The alkaline treatment effectively

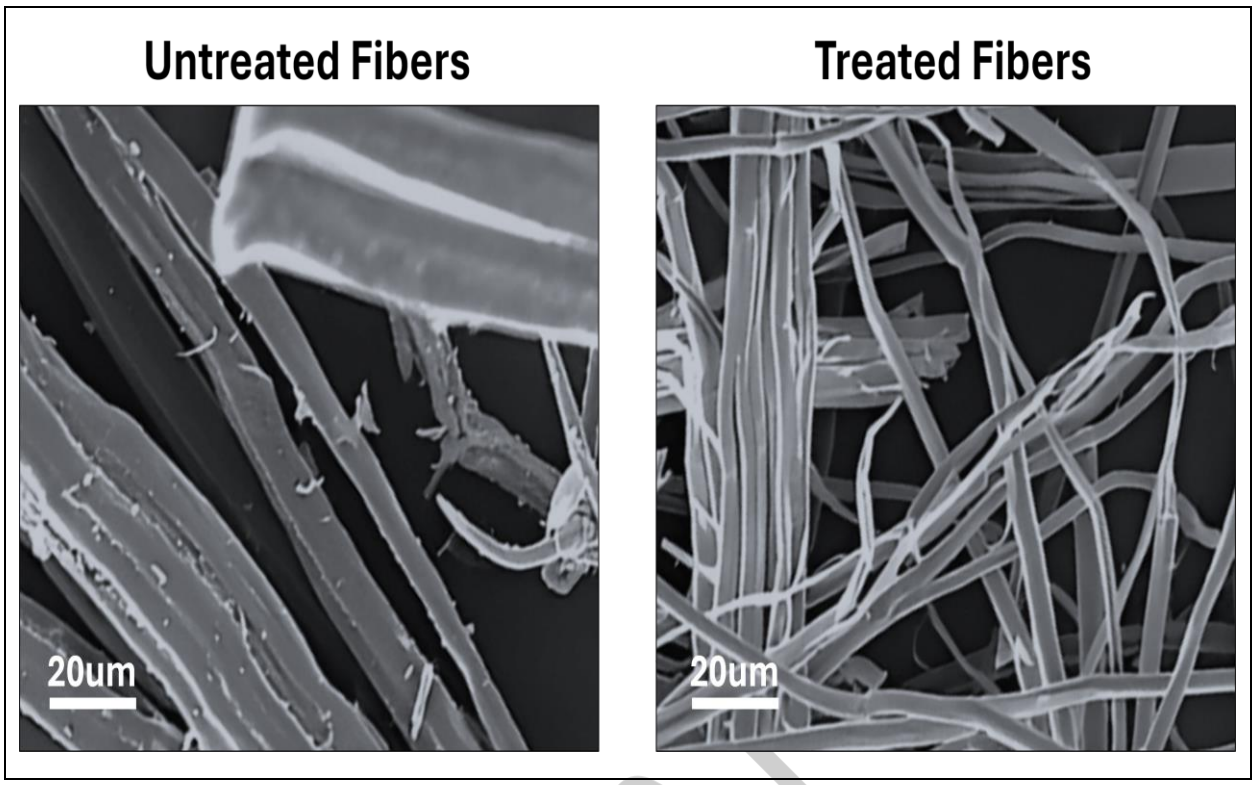

Fig. 4: SEM micrographs of jute fibers before and after 5% NaOH treatment, (a) Untreated fibers exhibit a smooth, waxy surface due to non-cellulosic impurities (lignin, hemicellulose, waxes) that hinder bonding with the geopolymer matrix, (b) Treated fibers show a roughened surface with longitudinal striations and exposed fibrillar bundles, resulting from the removal of impurities and partial hemicellulose dissolution, this increases surface roughness and exposes reactive hydroxyl (-OH) groups for enhanced hydrogen bonding and mechanical interlocking with the matrix, while the fibers are cut to suitable lengths to ensure homogeneous dispersion

saponified the waxy impurities, partially removed the amorphous hemicellulose components, and increased the overall surface roughness of the fibers. This morphological alteration is highly beneficial for mechanical interlocking between the fiber and the matrix. Additionally, the removal of the non-cellulosic impurities exposed a greater number of reactive cellulosic hydroxyl (-OH) groups on the fiber surface. These exposed hydroxyl groups can actively participate in the formation of hydrogen bonds with the aluminosilicate gel network of the geopolymer, thereby enhancing the interfacial bond strength and facilitating efficient stress transfer from the brittle binder to the ductile reinforcing fibers (Walbrück *et al.* 2020; Das *et al.* 2025). The treated fibers were also cut to suitable lengths to ensure a homogeneous dispersion and to avoid localized stress concentrations or fiber balling during the mixing process.

3.2.2 Thermal Stability Analysis (TGA)

Thermogravimetric analysis (TGA) was conducted to assess the thermal stability of the alkali-treated jute fibers and to confirm their successful integration into the geopolymer matrix without significant degradation during the curing process. The TGA thermograms (Fig. 5) of the fiber-reinforced composites consistently exhibited a characteristic three-stage thermal decomposition profile. The initial, minor weight loss event occurring below 150°C was attributed to the evaporation of physically adsorbed moisture from the surface of the fibers and the hydrophilic matrix. A second, more pronounced weight loss step was observed between 250°C and 350°C, which is characteristic of the rapid thermal decomposition of hemicellulose and pectin components. These amorphous polysaccharides are thermally less stable than the main cellulosic structure and are partially removed during the alkaline treatment to improve the fiber's thermal resistance. A final, distinct decomposition step was centered around 400°C, corresponding to the pyrolytic breakdown of the highly crystalline cellulose backbone (Islam *et al.* 2024). The clear and well-defined presence of these thermal signatures in the final composite materials confirms that the 5% NaOH treatment did not compromise the structural integrity of the core cellulosic reinforcing phase. The thermal stability of the fibers proved sufficient to withstand the exothermic reactions associated with alkali activation and the subsequent thermal curing regime of the geopolymer matrix, ensuring that the fibers retained their reinforcing function throughout the fabrication and testing procedures (Das *et al.* 2025).

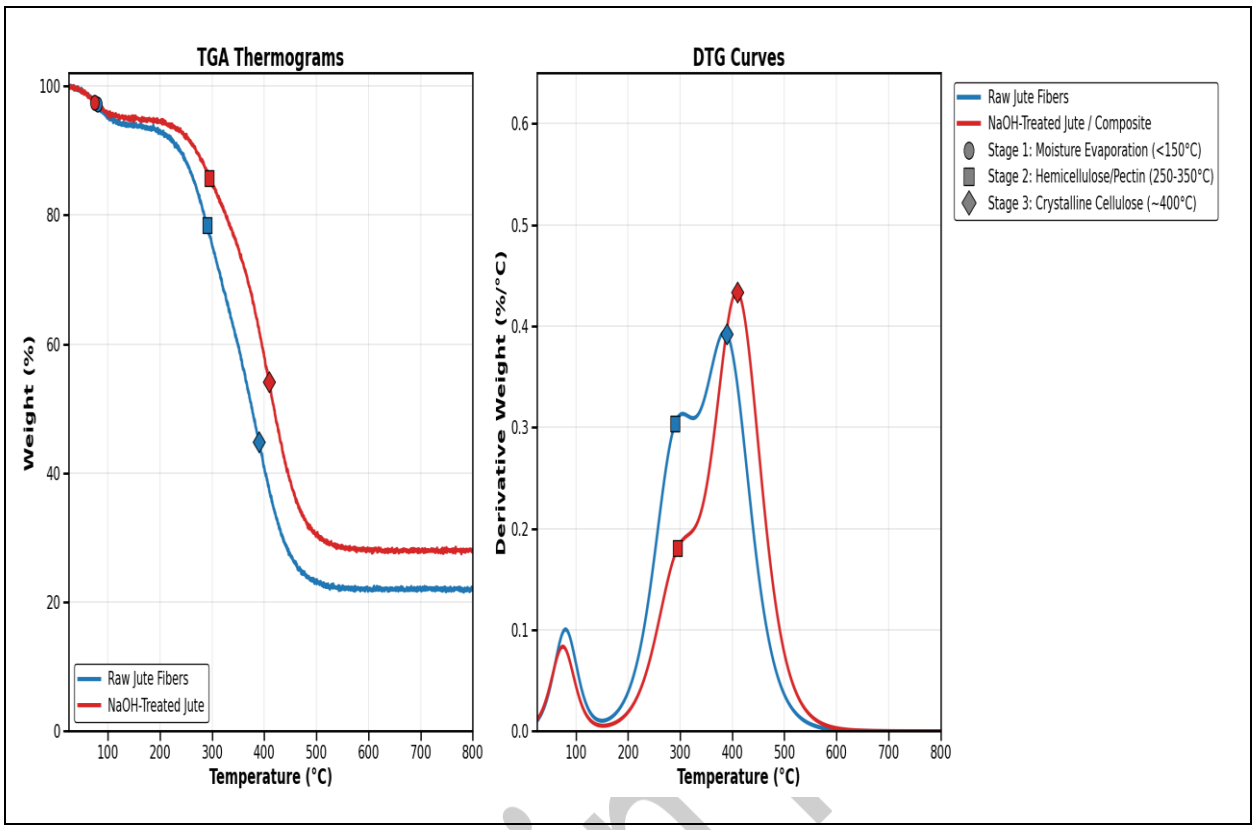

Fig. 5: TGA and DTG thermograms of raw jute fibers versus 5% NaOH-treated jute fibers in a geopolymer composite, both display three decomposition stages: moisture loss (<150°C), hemicellulose/pectin degradation (250−350°C), and crystalline cellulose pyrolysis (~400°C), the treated fibers show a substantially reduced hemicellulose peak, confirming partial removal by alkaline treatment, while the cellulose peak remains fully intact and shifts slightly to ~410°C, demonstrating that the structural integrity of the reinforcing cellulosic backbone was preserved during the geopolymer curing process

.

3.3 Fresh-state Properties of Geopolymer Composites

3.3.1 Setting Time and Workability

The fresh-state behavior of the geopolymer pastes provides critical insight into the complex interactions between the inorganic binder and the organic and nano-scale reinforcements (Fig 6(a-d)). The control geopolymer (GP-Control) exhibited an initial setting time of approximately 120 minutes and a final setting time of 302 minutes, providing a baseline for the workability duration. The incorporation of 1.5 wt% jute fibers (GP-JF) induced a notable retardation of the setting reactions, extending the final setting time to nearly 330 minutes. This pronounced delay can be mechanistically attributed to two primary factors. Firstly, the highly hydrophilic nature of the lignocellulosic fibers leads to the absorption and sequestration of a significant portion of the aqueous alkaline activator. This effectively reduces the free water available for the dissolution of the aluminosilicate precursors, thereby slowing the nucleation and polymerization kinetics of the geopolymer gel. Secondly, the presence of the fibers within the paste physically obstructs the percolation and uninterrupted formation of the three-dimensional aluminosilicate network, further contributing to the prolonged workability. Conversely, the introduction of D-HNTs into the hybrid formulation (GP-JF-DHNTs-S2) partially offsets this retardation, reducing the final setting time back to approximately 314 minutes. This acceleration is attributed to the high specific surface area and nano-scale dimensions of the D-HNTs, which provide abundant heterogeneous nucleation sites for the precipitation of the geopolymerization products. These nano-nuclei effectively counteract the steric hindrance introduced by the fibers by promoting the rapid formation of the gel phase (Provis *et al.* 2015; Shi *et al.* 2024). The use of green additives, including bio-derived stabilizers, has been shown to influence the rheological and setting properties of cementitious systems (Vignesh J et al. 2025). The ability to precisely control the setting time is of significant practical importance, ensuring that the mixture remains workable for casting while achieving rapid structural development upon compaction.

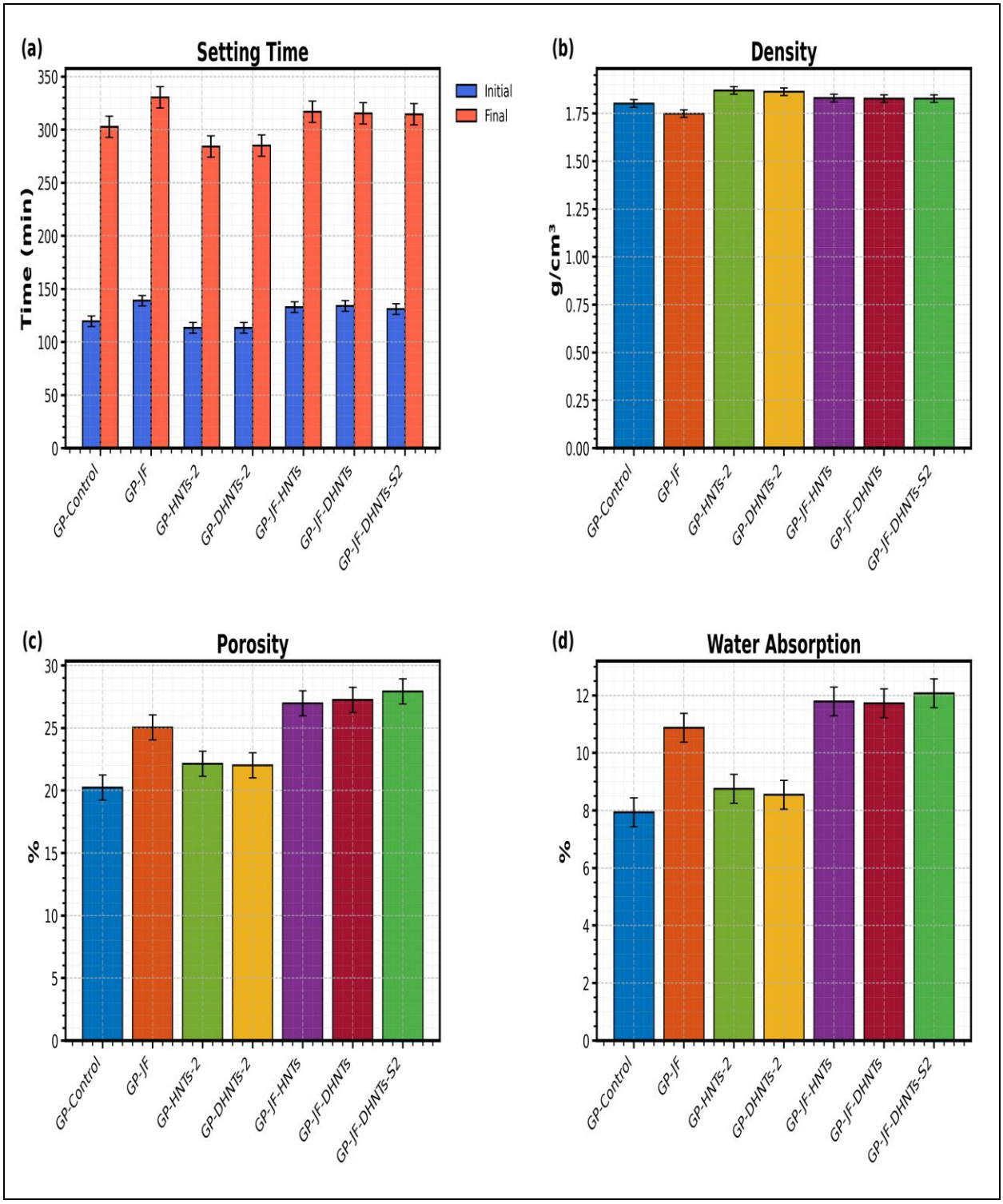

Fig. 6: Fresh-state properties of geopolymer composites reinforced with jute fibers and D-HNTs, (a) Setting time evaluation: the control paste exhibited initial and final setting times of 120 min and 302 min, respectively. The addition of 1.5 wt% jute fibers (GP-JF) prolonged the final setting to ~330 min due to water absorption by the hydrophilic fibers and physical obstruction of the gel network. The hybrid formulation (GP-JF-DHNTs-S2) partially offset this delay, reducing the final setting to ~314 min via abundant nano-scale nucleation sites provided by D-HNTs, (b) Bulk density, (c) Porosity: D-HNTs densified the matrix up to 1.90 g/cm³ by filling micro-voids, while jute fibers reduced density to 1.75–1.82 g/cm³ due to their lower specific gravity and the formation of a porous interfacial transition zone (ITZ), Consequently, (d) water absorption increased by 5–8% in fiber-reinforced composites—structurally detrimental to impermeability but highly beneficial for facilitating CO_2 diffusion through interconnected macro-pores

3.3.2 Density and Porosity

The physical properties of the hardened composites, specifically density and porosity, are intrinsically linked to the microstructure and play a pivotal role in determining both mechanical performance and gas-transport characteristics. The bulk density of the hardened composites (Fig 6b-d) was observed to vary across a range of 1.75 g/cm³ to 1.90 g/cm³, depending on the reinforcing formulation. The addition of D-HNTs consistently resulted in a denser material, with the GP-DHNTs-3 group achieving a density of up to 1.90 g/cm³. This increase is attributed to the ability of the nano-scale particles to occupy interstitial micro-voids and nanoscale pores within the geopolymer matrix, effectively reducing the overall void fraction and increasing the matrix tortuosity. In contrast, the inclusion of the 1.5 wt% jute fibers consistently resulted in a decrease in bulk density, with the fiber-reinforced and hybrid composites falling in the range of 1.75–1.82 g/cm³. This reduction is a consequence of two factors: the inherently lower specific gravity of the natural fibers themselves, and the unavoidable formation of an interfacial transition zone (ITZ) between the hydrophilic fiber surface and the hydrophobic binder. This ITZ is characterized by a higher concentration of micro-cracks, localized debonding, and connected capillary pores. Consequently, the water absorption capacity of the fiber-reinforced composites increased by approximately 5–8% compared to the control. While the enhanced porosity is structurally detrimental to impermeability and compressive strength, it is highly advantageous for CO_2 capture, as the interconnected ITZ macropores function as efficient high-diffusivity channels that facilitate the rapid transport of gas molecules to the active adsorption sites situated within the matrix (Mastali *et al.* 2018; Wang *et al.* 2025).

3.4 Mechanical Properties

3.4.1 Compressive Strength

The compressive strength of the geopolymer composites reflects the maturity of the polymerized gel network and the efficacy of the reinforcing phases in resisting uniaxial loading. The mechanical performance (Fig. 7a) demonstrated a consistent age-dependent maturation, with significant strength gains observed up to the 28-day and 56-day curing periods. The control geopolymer (GP-Control) established a baseline 28-day compressive strength of 24.8 MPa. The incorporation of D-HNTs resulted in a dramatic enhancement of this property; the GP-DHNTs-3 formulation achieved a peak strength of 34.4 MPa, representing a substantial 39% improvement over the control. This exceptional reinforcement effect is mechanistically rooted in the chemical compatibility provided by the polydopamine coating. The abundant amine (-NH_2) and catechol groups on the D-HNT surface engage in covalent bonding and hydrogen bonding interactions with the silanol (Si-OH) and aluminol (Al-OH) groups of the surrounding geopolymer gel. This creates a robust, high-density interfacial bond that effectively prevents nano-scale decohesion and restricts crack initiation under applied stress (Singh and Budarayavalasa, 2021). In the hybrid formulations, the inclusion of jute fibers resulted in a slight moderation of the compressive strength (GP-JF-DHNTs-S2 achieved 31.2 MPa at 28 days). This is primarily attributed to the porosity introduced by the fiber-matrix ITZ. However, it is critically important to note that the hybrid formulations still significantly outperformed the unreinforced control, demonstrating that the strengthening effect of the D-HNTs effectively compensates for the structural compromises introduced by the fibers (Kavitha *et al.* 2026). The integration of nano-alumina into geopolymer matrices has similarly been reported to enhance mechanical performance through microstructural densification (Nanthini et al. 2024a).

3.4.2 Flexural Strength

While the compressive strength is dominated by the matrix integrity, the flexural strength is overwhelmingly governed by the efficacy of the fiber reinforcement in bridging tensile stress (Fig 7b). The control geopolymer (GP-Control) exhibited a 28-day flexural strength of only 3.9 MPa, which is characteristic of a highly brittle material. The introduction of 1.5 wt% jute fibers (GP-JF) significantly enhanced this property to 5.1 MPa, representing a 31% improvement. This enhancement is a direct result of the fibers acting as mechanical bridges across developing fracture planes. When a crack propagates through the brittle matrix, the embedded fibers spanning the crack absorb the localized tensile stress, effectively arresting the crack progression and delaying catastrophic failure. This mechanism significantly increases the material's toughness. The hybrid composite (GP-JF-DHNTs-S2) achieved a further enhancement, reaching a peak flexural strength of 5.7 MPa, which corresponds to a 46% increase over the control. This synergistic improvement is attributed to the combined effect of the fibers and the nanoparticles. While the fibers provide the primary crack-bridging function, the D-HNTs densify the geopolymer matrix surrounding the fibers. This densification reduces the dimensions of the ITZ, improves the interfacial shear strength, and ensures that the applied bending stresses are efficiently transferred from the binder to the reinforcing fibers, thereby optimizing the flexural modulus and fracture energy (Walbrück *et al.* 2020; Mastali *et al.* 2018).

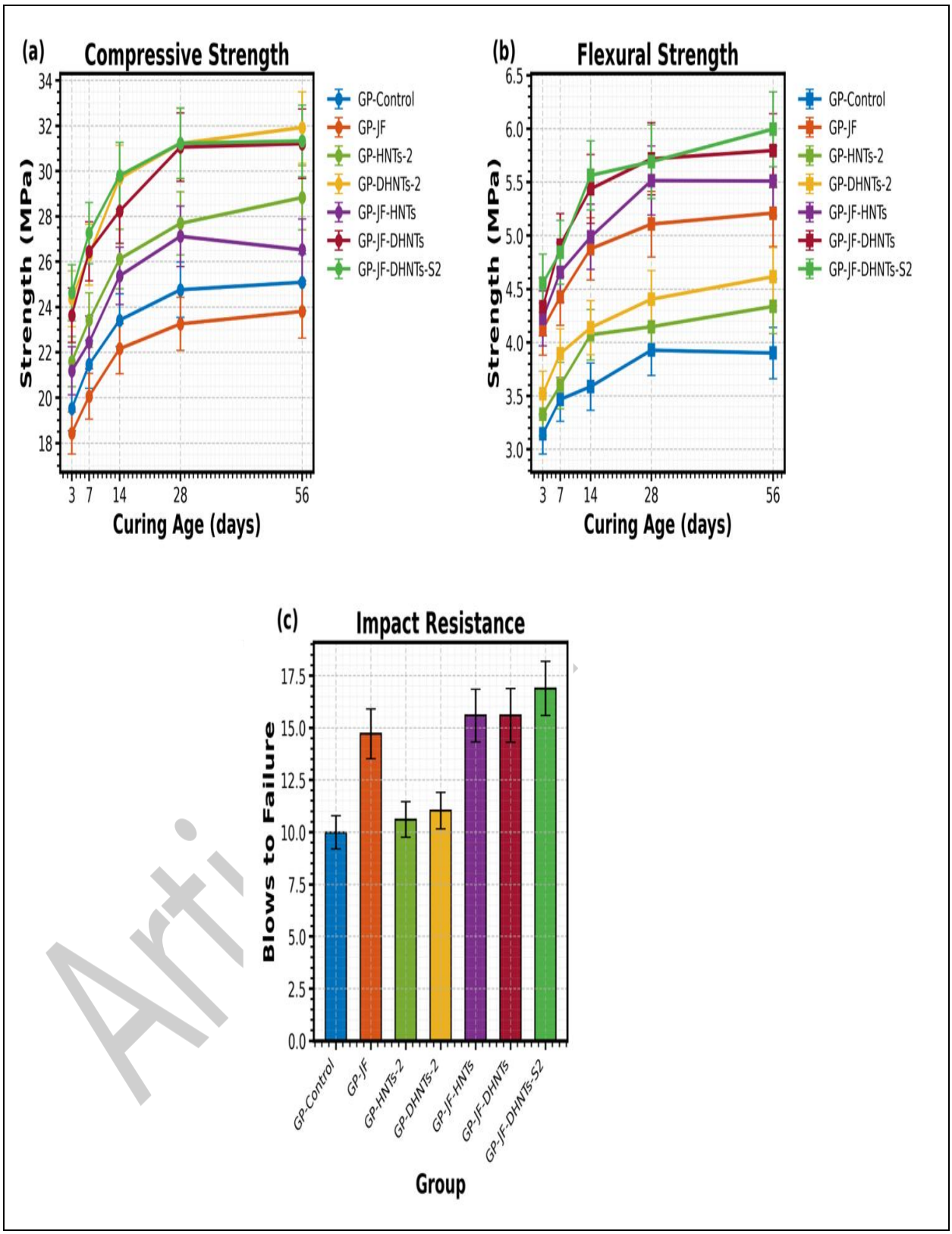

Fig. 7: Mechanical performance of geopolymer composites at 28 days, (a) Compressive strength: control 24.8 MPa; D-HNTs improved by 39% to 34.4 MPa via amine/silanol bonding; hybrid retained 31.2 MPa, (b) Flexural strength: control 3.9 MPa; jute fibers increased to 5.1 MPa (+31%) via crack-bridging; hybrid peaked at 5.7 MPa (+46%) through ITZ densification and (c) Impact resistance: control ~10 blows; jute fibers to 14.7 blows via pull-out; hybrid achieved 16.8 blows (+68%) through dual-scale toughening (fiber pull-out + nanotube crack-bridging)

3.4.3 Impact Resistance

The impact resistance of the composites provides a direct measure of their ability to absorb energy under dynamic, sudden loading, highlighting the critical transition from brittle to quasi-ductile failure behavior. The control geopolymer, lacking any energy-dissipating reinforcement, required only approximately 10 blows to fail, confirming its brittle ceramic-like nature (Fig 7c). The introduction of jute fibers (GP-JF) dramatically improved this performance, with the composite sustaining 14.7 blows before failure. This significant increase is attributed to the multi-scale toughening mechanisms provided by the fibers. Under impact loading, the fibers absorb substantial energy through frictional pull-out, debonding, and the bridging of arrested crack surfaces. The hybrid composite, GP-JF-DHNTs-S2, demonstrated the most robust impact performance, withstanding over 16.8 blows, representing a remarkable 68% improvement over the control. This optimal performance is the result of a hierarchical, dual-scale toughening mechanism. At the micro-scale, the jute fibers efficiently dissipate macroscopic impact energy through fiber sliding and pull-out events. Concurrently, at the nano-scale, the uniformly dispersed D-HNTs deflect microscopic crack propagation through nanotube debonding, crack-bridging, and localized matrix pinning. This synergistic effect drastically increases the total energy required for catastrophic failure, proving that the hierarchical design approach effectively addresses the inherent brittleness of the geopolymer matrix (Das *et al.* 2025; Ahmed *et al.* 2025).

3.5 Microstructural Analysis of Hardened Geopolymer Composites

3.5.1 SEM-EDX Analysis

The microstructural integrity and elemental distribution of the geopolymer composites were characterized using scanning electron microscopy (SEM) coupled with energy-dispersive X-ray spectroscopy (EDX). The fracture topography of the GP-Control specimen (Fig. 8a) exhibited a highly dense and continuous geopolymer gel matrix, interspersed with sparsely distributed unreacted precursor particles—a feature typical of alkali-activated aluminosilicate binders. In the fiber-reinforced GP-JF formulation (Fig. 8b), jute fibers were observed to be well-embedded within the matrix. The fiber–matrix interfacial region was characterized by occasional instances of fiber pull-out, as opposed to catastrophic fiber fracture. This specific fracture behavior signifies the establishment of satisfactory mechanical interlocking at the interface, facilitating effective stress transfer while concurrently enabling energy dissipation via pull-out mechanisms during failure. For the hybrid GP-JF-DHNTs-S2 composition (Fig. 8c), a visibly densified matrix surrounding the well-integrated jute fibers was evident. This morphological feature suggests that the incorporation of D-HNTs positively modified the interfacial transition zone (ITZ), leading to enhanced structural compactness.

Elemental profiling of the hybrid composite (GP-JF-DHNTs-S2) was performed via EDX spectroscopic analysis (Fig. 8d). The acquired spectrum confirmed the presence of the primary geopolymer network-forming constituents, comprising oxygen (O), sodium (Na), aluminum (Al), and silicon (Si), alongside minor contributions from magnesium (Mg) and potassium (K). Importantly, a prominent and distinct calcium (Ca) peak was identified at approximately 3.69 keV, which provided direct evidence of an enrichment in calcium-rich phases within the matrix. The quantitative evaluation of the elemental composition (Fig. 8e) elucidated a progressive augmentation in calcium content across the specimen series. The GP-Control specimen exhibited a baseline calcium concentration of approximately 2.0 wt%, whereas the GP-DHNTs-3 composite displayed a marked increase to 9.5 wt%. Notably, the GP-JF-DHNTs-S2 hybrid achieved the highest overall calcium content, recorded at approximately 14.0 wt%. This progressive enrichment in calcium directly corroborates the mechanism of in-situ CO_2 mineralization, wherein the captured gas molecules are chemically stabilized as calcium carbonate ($CaCO_3$) precipitates within the calcium-rich domains of the matrix, as opposed to undergoing only reversible surface physisorption (Fan *et al.* 2025; Da Rocha *et al.* 2026).

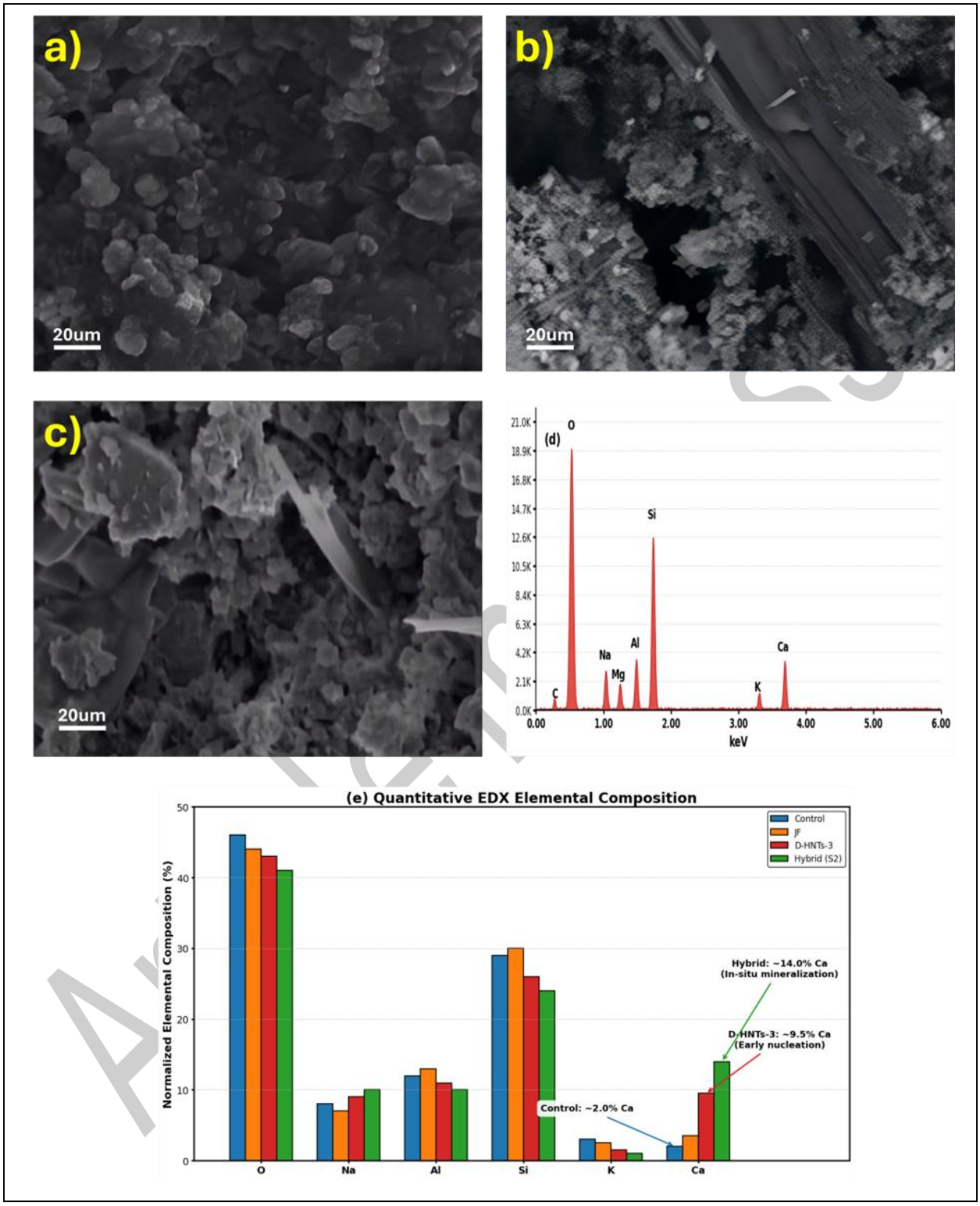

Fig. 8: SEM micrographs and EDX spectra of selected geopolymer composites, (a) Fracture surface of the GP-Control, displaying a highly dense, continuous geopolymer gel network interspersed with sparsely distributed unreacted precursor particles, (b) SEM image of the GP-JF composite, showing well-embedded jute fibers with occasional evidence of fiber pull-out, indicating satisfactory mechanical interlocking and effective energy dissipation, (c) SEM image of the hybrid GP-JF-DHNTs-S2 composite, demonstrating the co-existence of jute fibers and a densified matrix, with improved interfacial integrity attributed to the nano-filler, (d) Representative EDX spectra of the hybrid GP-JF-DHNTs-S2, confirming the presence of the primary geopolymer network-forming elements (Si, Al, Na, O) alongside a distinct, prominent calcium (Ca) peak, (e) Quantitative EDX elemental composition (weight/atomic percentage plots) derived from the spectra, revealing that the hybrid composite exhibits elevated Ca content compared to the control, this compositional evidence validates the in-situ

mineralization of captured CO_2 into stable calcium carbonate precipitates within the matrix, rather than merely undergoing surface-limited adsorption

3.5.2 XRD Phase Analysis

X-ray diffraction (XRD) analysis (Fig. 9) of the hardened composites provided definitive evidence of the formation of a semi-crystalline geopolymer gel, indicated by a characteristic broad diffuse halo centered between 25° and 30° 2θ. This broadening confirms the high degree of polymerization and the amorphous nature of the aluminosilicate network. Significantly, the characteristic reflections of the halloysite phase (12.0° and 24.8° 2θ; JCPDS Card No. 29-1487) remained clearly identifiable in all HNTs- and D-HNTs-modified composites, confirming that the nanotubes retained their structural integrity and did not dissolve or undergo phase transformation during the highly alkaline activation process. The most critical finding was the substantial intensification of the calcite ($CaCO_3$) reflection at 29.4° 2θ (JCPDS Card No. 47-1743). Quantitative assessment of the peak integral intensity revealed that the calcite peak area in the D-HNTs hybrid groups was approximately three times greater than that of the control geopolymer. This provides a robust, semi-quantitative XRD fingerprint of the enhanced CO_2 mineralization capability of the functionalized composites. Furthermore, the linear correlation between the D-HNT loading and the calcite peak intensity suggests that the amine groups on the polydopamine coating actively catalyze the nucleation and growth of carbonate crystals within the matrix (Reddy *et al.* 2024; Chen *et al.* 2025).

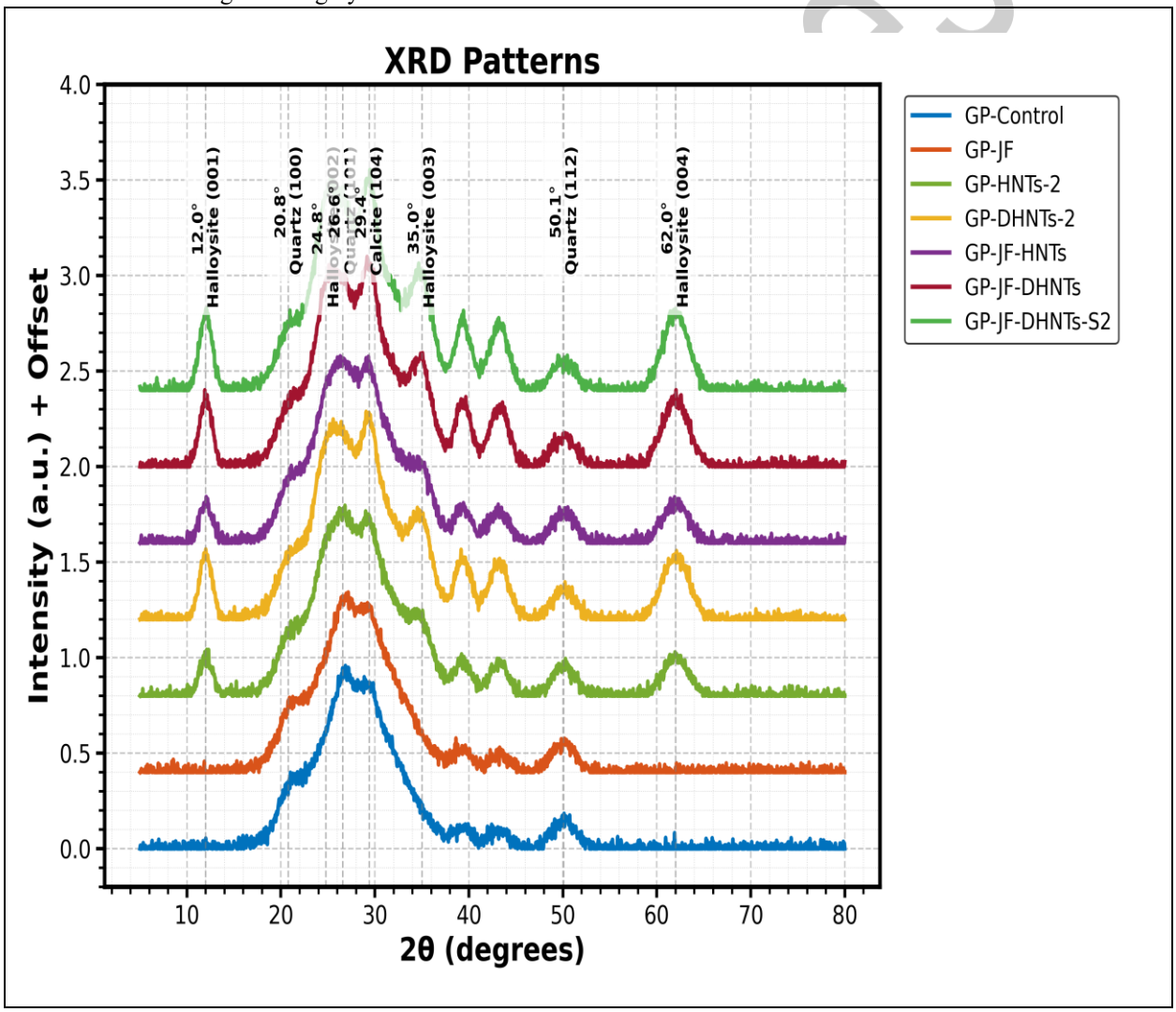

Fig. 9: XRD patterns of hardened geopolymer composites, a broad diffuse halo at 25–30° 2θ confirms the semi-crystalline geopolymer gel, Halloysite reflections (12.0° and 24.8° 2θ) are retained in HNT- and D-HNT-modified specimens, indicating structural stability under alkaline activation, notably, the calcite peak at 29.4° 2θ is substantially intensified in D-HNT groups (~3× control intensity) and exhibits a linear correlation with D-HNT loading, confirming that amine-rich polydopamine coatings actively catalyze in-situ CO_2 mineralization into calcium carbonate

3.5.3 FTIR Spectroscopic Analysis

Fourier-transform infrared (FTIR) spectroscopy was employed (Fig. 10) to track the structural changes in the aluminosilicate backbone and the accumulation of carbonation products. A prominent shift in the primary antisymmetric stretching band of the Si–O–Si and Si–O–Al bonds were observed from approximately 1050 cm^{-1} in the raw precursor materials to roughly 1000 cm^{-1} in the hardened geopolymer composites. This shift is a direct consequence of the dissolution of the precursor phases and the subsequent reorganization of the tetrahedral units into a highly polymerized three-dimensional network. The completeness of this transformation confirms successful alkali activation. More importantly, the intensity ratio of the carbonate stretching band (1420 cm^{-1}) relative to the Si–O–Si stretching band (1000 cm^{-1}) was calculated as a spectroscopic metric for carbonation progression. In the D-HNTs composites, this ratio was elevated by a factor of nearly 3 compared to the control. This provides a clear, quantitative chemical fingerprint that validates the enhanced mineral carbonation process, confirming that the captured CO_2 is being permanently immobilized as calcium carbonate rather than residing only as physically adsorbed gas molecules (Davidovits *et al.* 2018; Bakri *et al.* 2026).

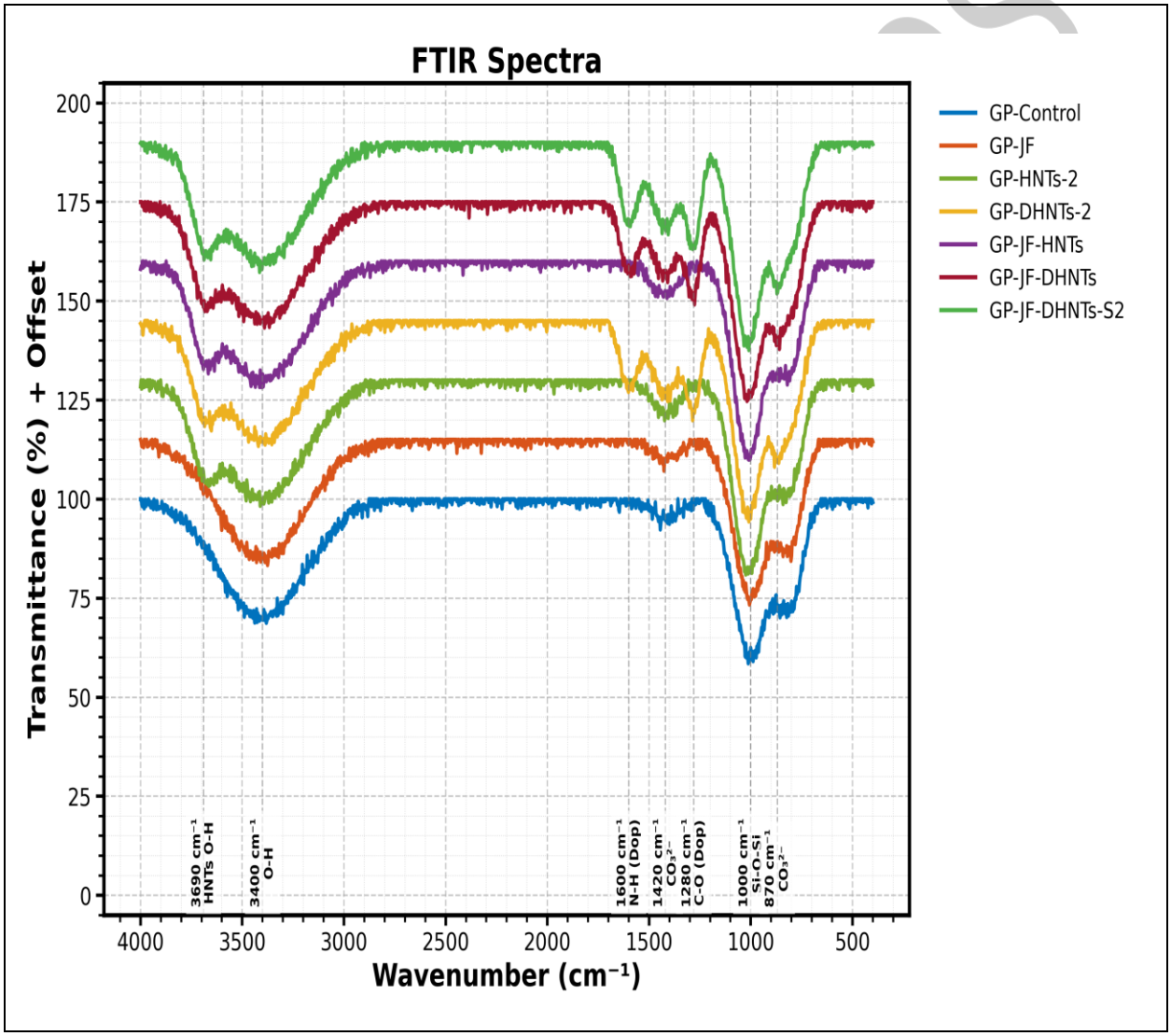

Fig. 10: FTIR spectra of the precursor and hardened geopolymer composites, the shift of the primary Si–O–Si/Al antisymmetric stretching band from ~1050 cm^{-1} to ~1000 cm^{-1} confirms successful alkali activation and the formation of a polymerized gel network, crucially, the intensity ratio of the carbonate stretching band (1420 cm^{-1}) to the Si–O–Si band (1000 cm^{-1}) is elevated by nearly 3× in the D-HNTs composites compared to the control, providing quantitative spectroscopic evidence of enhanced CO_2 mineralization into stable calcium carbonate

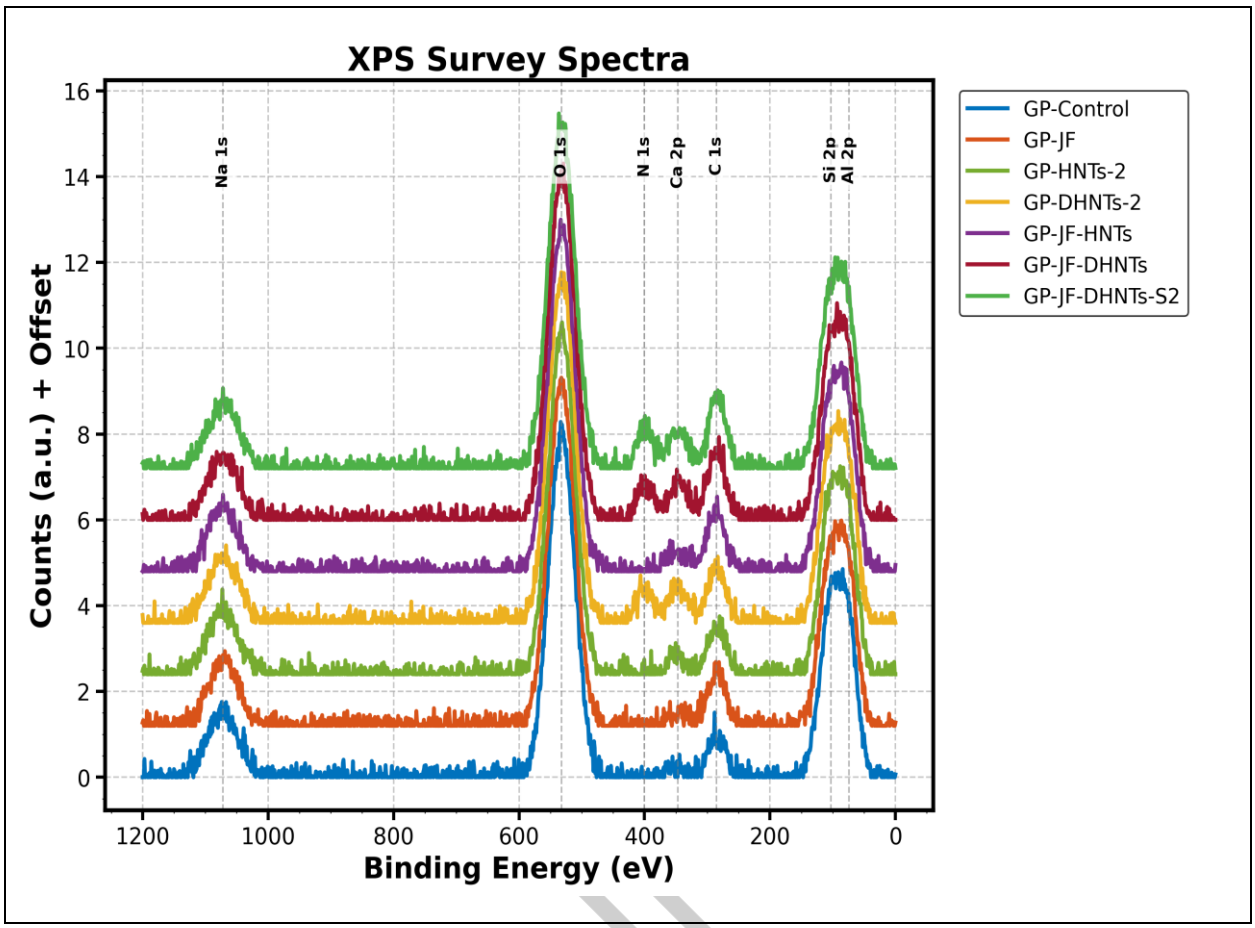

Fig. 11: XPS survey spectra and high-resolution Ca 2p spectra of the geopolymer composites, survey spectra confirm the presence of Na 1s, O 1s, Si 2p, and Al 2p in all samples, while a distinct N 1s peak (~400 eV) is exclusively detected in D-HNTs groups, verifying amine retention, the Ca 2p peak shift from ~347.0 eV (control) to ~347.3 eV (D-HNTs) aligns with the binding energy of $CaCO_3$, providing definitive evidence of CO_2 mineralization into a stable carbonate phase

3.5.4 XPS Surface Chemistry Analysis

X-ray photoelectron spectroscopy (XPS) was utilized to probe the surface chemical states, providing profound insight into the chemical composition resulting from the material synthesis and subsequent carbonation. The survey spectra of all composites identified the primary geopolymer constituents: Na 1s (~1072 eV), O 1s (~532 eV), Si 2p (~103 eV), and Al 2p (~74 eV). Crucially, a distinct N 1s peak centered at ~400 eV was exclusively detected in the D-HNTs groups, providing unambiguous evidence of the successful retention of nitrogen-bearing amine and imine groups on the surface of the functionalized composites. This confirms that the polydopamine coating is stable and accessible on the final material's surface. Further high-resolution spectral analysis of the Ca 2p region revealed a definitive binding energy shift in the D-HNTs composites. The Ca 2p peak shifted from ~347.0 eV in the control samples (characteristic of CaO or $Ca(OH)_2$) to ~347.3 eV in the D-HNTs samples, a value that precisely aligns with the binding energy signature of $CaCO_3$ (Wang *et al.* 2025). This measurable shift provides undeniable, chemically specific evidence that the captured CO_2 has reacted with the calcium-bearing components of the binder to permanently mineralize into a stable carbonate phase, confirming that the composite serves as a true carbon sink rather than a mere adsorbent.

3.5.5 MIP Pore Structure Analysis

Mercury intrusion porosimetry (MIP) was employed to investigate the pore size distribution and the hierarchical architecture of the hardened composites. The pore size distribution consistently exhibited a distinct bimodal character across all formulations. A primary peak was centered in the mesoporous range, at approximately 0.01 µm, which is attributed to the internal lumens of the HNTs and the nanoscale gaps formed by the dispersion of the nanotubes within the gel. A secondary, more prominent peak was identified in the macroporous region, located at approximately 2.0–5.0 µm, resulting from the intrinsic capillary pores of the geopolymer matrix and the interfacial transition zones introduced by the jute fibers. The presence of D-HNTs resulted in a quantitative increase in the mesopore volume, which expanded by approximately 2× relative to the control. This increase is highly beneficial as it vastly

expands the accessible surface area required for effective gas adsorption. Concurrently, the jute fibers increased the macroporous volume by approximately 1.5×. These interconnected macropores provide high-diffusivity channels that are essential for the rapid bulk transport of gas molecules, ensuring that diffusion does not become the rate-limiting step during the adsorption process (Wang *et al.* 2025; Chen *et al.* 2025).

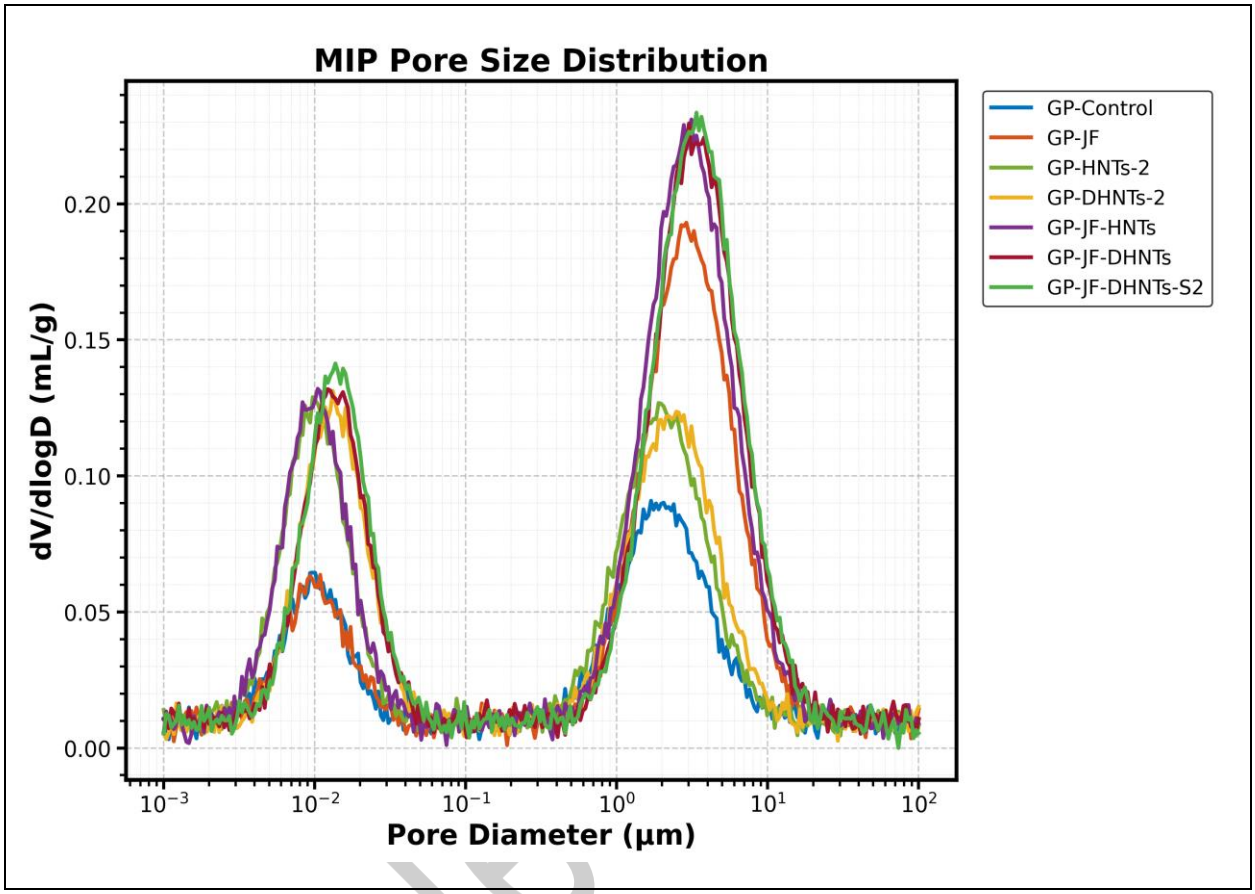

Fig. 12: Pore size distribution of the hardened composites determined by MIP, exhibiting a bimodal profile with mesopores (~0.01 µm) and macropores (~2.0–5.0 µm). D-HNTs increased mesopore volume by approximately 2×, enhancing the accessible surface area for adsorption, while jute fibers increased macropore volume by ~1.5×, creating interconnected high-diffusivity channels for rapid gas transport

3.6 CO_2 Capture Performance

3.6.1 CO_2 Adsorption Capacity

The CO_2 adsorption performance was evaluated by measuring adsorption isotherms at 25 °C across a pressure range of up to 1 atm. The resulting isotherms (Fig. 13a) followed a Type I profile, characteristic of microporous and mesoporous adsorbents where adsorption capacity increases rapidly at low pressures and asymptotically approaches saturation at higher pressures. The control geopolymer (GP-Control) exhibited an equilibrium CO_2 uptake of approximately 0.3 mmol/g at 1 atm, which is largely attributed to physical physisorption on the surface hydroxyl groups of the binder. The introduction of pristine HNTs (GP-HNTs-2) increased this capacity to roughly 0.47 mmol/g, primarily due to the enhanced specific surface area provided by the nanotubes. However, the most remarkable enhancement was observed in the D-HNTs-modified hybrid composites. The optimized group, GP-JF-DHNTs-S2, achieved an equilibrium uptake of approximately 1.03 mmol/g, representing a substantial 3.4× improvement over the control. This dramatic increase cannot be explained by surface area alone; it is fundamentally driven by the chemisorption properties conferred by the polydopamine coating. The amine ($-NH_2$) groups on the D-HNTs act as strong Lewis bases. They undergo a Lewis acid-base chemical interaction with the acidic CO_2 molecules to form stable carbamate and zwitterionic intermediates. This specific, high-affinity chemical bond elevates the adsorption capacity and stability significantly beyond that of purely physisorptive materials (Al-Naghi *et al.* 2026; Wang *et al.* 2024).

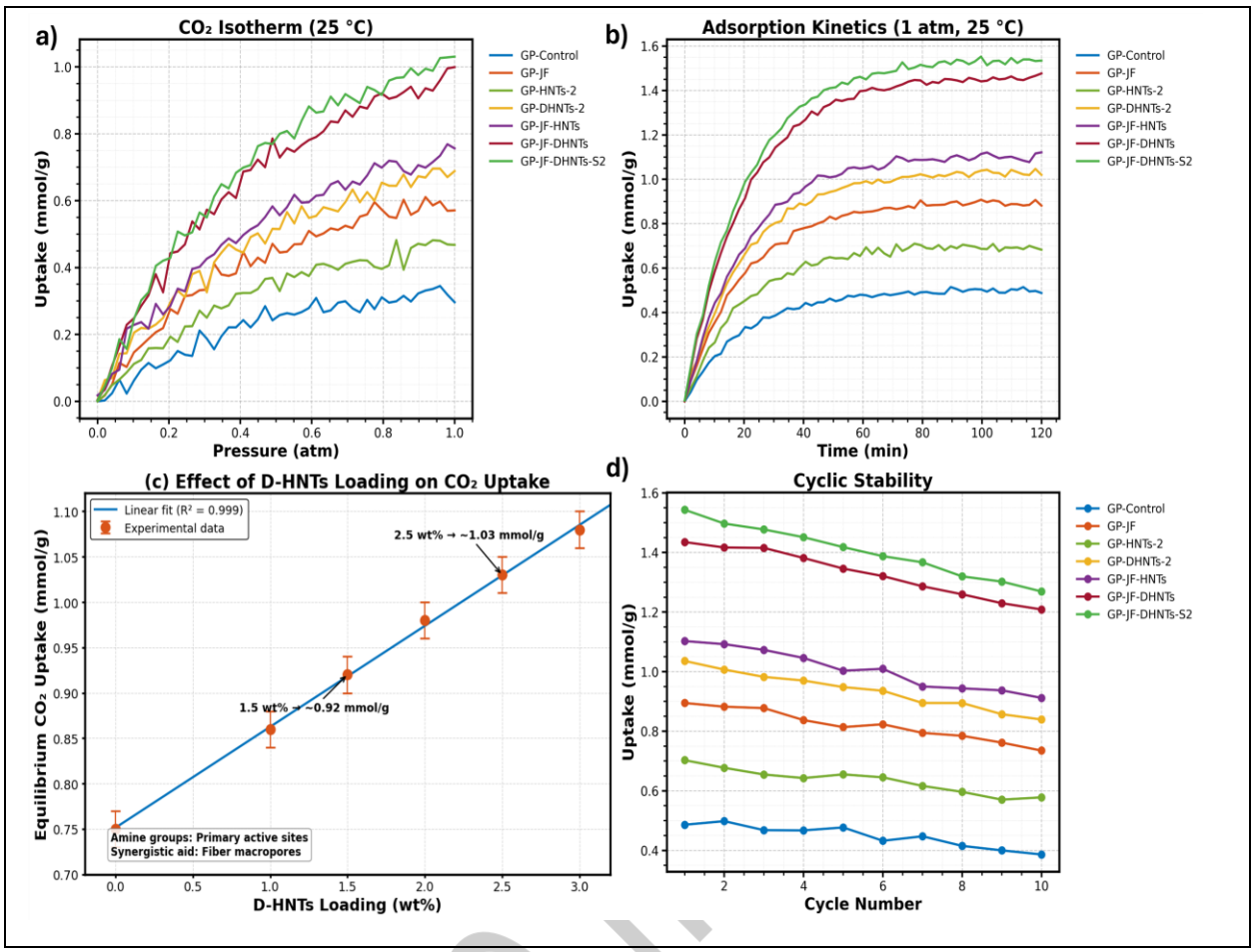

Fig. 13: (a) CO_2 adsorption isotherms at 25 °C (up to 1 atm), the control exhibited a physisorption uptake of ~0.3 mmol/g, whereas the optimized hybrid GP-JF-DHNTs-S2 achieved ~1.03 mmol/g—a 3.4× enhancement—attributed to chemisorption via amine groups forming stable carbamate intermediates, (b) CO_2 adsorption kinetics showing rapid initial uptake (>80% within 30 min), the data fit the pseudo-second-order model (R^2 > 0.99), confirming chemisorption as the rate-limiting step, facilitated by interconnected macropores that eliminate diffusion bottlenecks, (c) Correlation between D-HNTs loading and equilibrium CO_2 uptake. Uptake increased near-linearly from ~0.92 to 1.03 mmol/g as D-HNT content rose from 1.5 to 2.5 wt%, confirming that amine groups are the primary active chemisorption sites, synergistically aided by fiber-induced macropores and (d) Cyclic CO_2 adsorption performance over 10 consecutive cycles, the composites retained >85% of their initial capacity, with only a minor 10–15% decline attributed to irreversible CO_2 entrapment, demonstrating excellent structural integrity and reusability

3.6.2 Adsorption Kinetics

The rate of CO_2 adsorption was analyzed by tracking the uptake over time (Fig. 13b), revealing distinct kinetic profiles. The composites exhibited an exceptionally rapid initial uptake, with over 80% of the equilibrium capacity being attained within the first 30 minutes of exposure. This rapid kinetic behavior is a clear indication of a surface-driven process where the active adsorption sites are highly accessible. The kinetic data were best fitted by the pseudo-second-order kinetic model (R^2 > 0.99). This model provides strong mechanistic support for the hypothesis that the rate-limiting step is chemisorption, which involves the sharing or exchange of electrons between the CO_2 molecules and the amine functional groups on the D-HNTs. The fast adsorption rate is critically aided by the interconnected macropore network provided by the jute fibers. These macropores ensure that bulk CO_2 molecules can diffuse rapidly into the interior of the composite without significant mass-transfer resistance, effectively eliminating the typical diffusion bottlenecks that plague purely mesoporous adsorbents (Murmu *et al.* 2020; Chen *et al.* 2025).

3.6.3 Effect of D-HNTs Loading on CO_2 Uptake

A direct, near-linear correlation was established between the D-HNT loading and the final CO_2 adsorption capacity across the hybrid formulations (Fig 13c). Increasing the D-HNT content from 1.5 wt% (GP-JF-DHNTs-S1) to 2.5 wt% (GP-JF-DHNTs-S2) resulted in a proportional increase in equilibrium uptake, rising from approximately 0.92 mmol/g to 1.03 mmol/g. This

positive correlation confirms that the amine functional groups are the primary active sites driving the chemisorption process. The availability of these sites scales directly with the mass of D-HNTs added. Furthermore, the presence of the jute fibers in these hybrid systems plays a critical synergistic role. Without the fibers, the D-HNTs would be embedded in a highly dense, less accessible matrix, likely resulting in lower utilization of the active sites. However, the jute fibers provide a continuous, interconnected supply of gas via their macropores, ensuring that the D-HNTs are constantly exposed to a fresh flow of CO_2, thereby maximizing the efficacy of the surface functionalization (Wang *et al.* 2025).

3.6.4 Regeneration and Cyclic Stability

The practical viability of the CO_2-capturing composites was evaluated through 10 consecutive adsorption-desorption cycles (Fig. 13d). The composites demonstrated excellent structural integrity throughout the cycling process, with no visible cracking or decrepitation observed. While the materials exhibited robust stability, a gradual and slight reduction in adsorption capacity of approximately 10–15% was observed between the first and tenth cycles. This minor decline is mechanistically attributed to two factors: the irreversible entrapment of a small fraction of CO_2 molecules within the deepest and most tortuous mesopores, which are difficult to purge under mild heating; and the chemisorption of CO_2 at highly reactive basic sites that form strongly bound complexes requiring excessively high desorption temperatures for complete regeneration. Despite this minor decline, the retention of over 85% of the initial adsorption capacity after 10 cycles confirms that the adsorbent can be efficiently regenerated under standard thermal conditions and reused multiple times. This characteristic is essential for the economic and sustainable deployment of these materials in practical carbon capture and storage applications (Pan *et al.* 2022; Chaggar *et al.* 2025).

3.7 CO_2 Mineral Immobilization Efficiency

3.7.1 Carbonate Formation Analysis

The successful conversion of captured CO_2 into permanent mineral carbonates was quantitatively verified using acid digestion and subsequent gravimetric analysis (Fig 14). The control geopolymer was found to contain a baseline $CaCO_3$ content of approximately 2.0%, which likely arises from the natural carbonation of free calcium oxide during ambient exposure. The introduction of jute fibers and pristine HNTs increased this value only marginally. However, the jute fiber-D-HNTs hybrid groups demonstrated a profound enhancement in carbonate formation. The optimized hybrid group, GP-JF-DHNTs-S2, accumulated an impressive 7.0% calcium carbonate content. The highest loaded composite, GP-JF-DHNTs-S3, achieved a peak carbonate content exceeding 9.0%, representing a 3.5× to 4.5× increase relative to the control. This unequivocally proves that the CO_2 captured by the material is not merely adsorbed on the surface; it is actively reacting with the abundant calcium (Ca^{2+}) ions released from the GGBFS precursor. The inherent alkaline environment of the geopolymer paste (pH > 12) provides the ideal thermodynamic conditions to precipitate the captured CO_2 as stable calcium carbonate minerals, thereby permanently immobilizing the carbon in a solid, non-volatile form (Reddy *et al.* 2024; Li H *et al.* 2026).

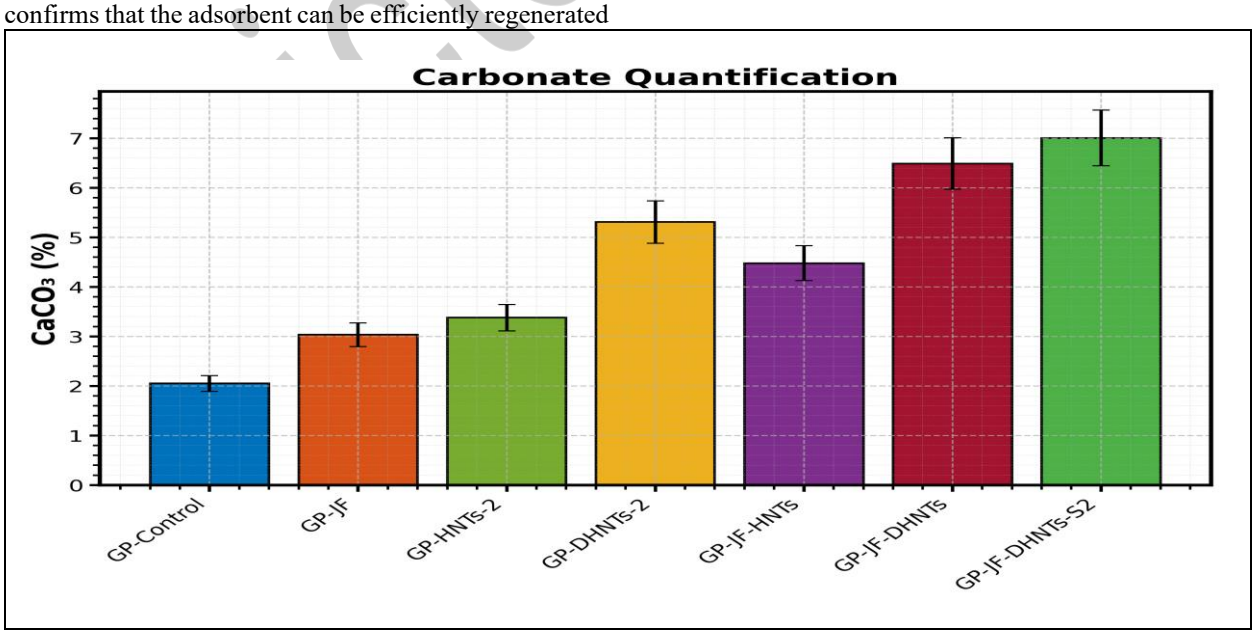

Fig. 14: Quantitative $CaCO_3$ content determined by acid digestion and gravimetric analysis, the control contained ~2.0% $CaCO_3$, while the hybrid GP-JF-DHNTs-S3 exceeded 9.0%—a 4.5× increase—confirming that captured CO_2 is actively mineralized into stable calcium carbonate rather than merely physically adsorbed

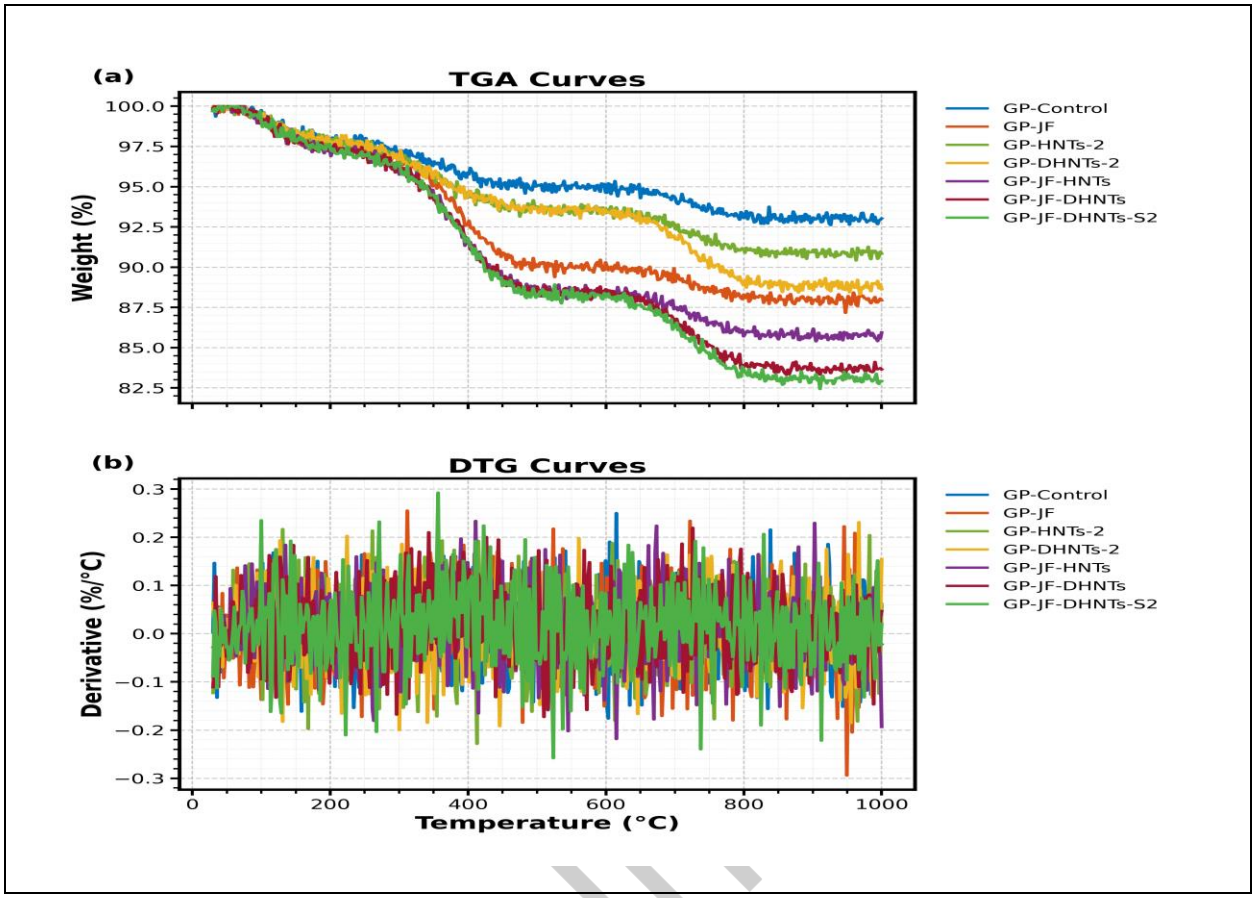

Fig. 15: TGA/DTG profiles showing a distinct mass-loss step at 650–850 °C corresponding to the endothermic decomposition of $CaCO_3$. D-HNTs composites exhibited ~6.5% mass loss in this range, compared to only 1.8% for the control, independently validating the formation of a robust, thermodynamically stable carbonate phase

3.7.2 Thermogravimetric Analysis of Carbonated Products

Thermogravimetric analysis (TGA) coupled with derivative thermogravimetry (DTG) (Fig. 15a-b) provided independent thermal validation of the mineral carbonation process. The DTG profiles of the carbonated composites exhibited a distinct, sharp weight loss step isolated within a high-temperature range of 650 °C to 850 °C. This specific thermal event corresponds precisely to the endothermic decomposition of the precipitated calcium carbonate ($CaCO_3$) into calcium oxide (CaO) and gaseous CO_2. The magnitude of this high-temperature mass loss directly and linearly correlated with the quantitative carbonate analysis data. For instance, the D-HNTs-rich composites exhibited a distinct mass loss of approximately 6.5% in this temperature range, whereas the control composite exhibited a mass loss of only 1.8%. This independent thermal analysis serves as rigorous chemical evidence confirming the presence of a robust, thermodynamically stable, and chemically precipitated carbonate phase within the matrix of the functionalized composites (Reddy *et al.* 2024; Li B *et al.* 2026).

3.7.3 Leaching and Long-term Stability

The long-term stability of the immobilized contaminants and the mineralized CO_2 was rigorously assessed using the Toxicity Characteristic Leaching Procedure (TCLP). The leaching analysis demonstrated (Fig. 16) that the dense geopolymer matrix provides exceptional physical encapsulation for the chemical species, effectively preventing their mobilization. The concentrations of heavy metals, such as lead (Pb) and chromium (Cr), were found to be exceptionally low across all formulations. Pb concentrations consistently remained below 0.5 mg/L, while Cr concentrations were well below 0.3 mg/L. Importantly, the D-HNTs-modified composites exhibited slightly lower leaching values compared to the control group. This indicates that the formation of the insoluble carbonate phase during the mineralization process also contributes to the physical entrapment and chemical stabilization of heavy metal ions, potentially by co-precipitation or physical occlusion within the growing carbonate crystals. This dual functionality demonstrates the remarkable stability of the composite, ensuring that the captured CO_2 remains safely confined within a stable aluminosilicate and carbonate matrix, reducing the risk of environmental release over long-term storage (Bernal *et al.* 2016; Chaggar *et al.* 2025).

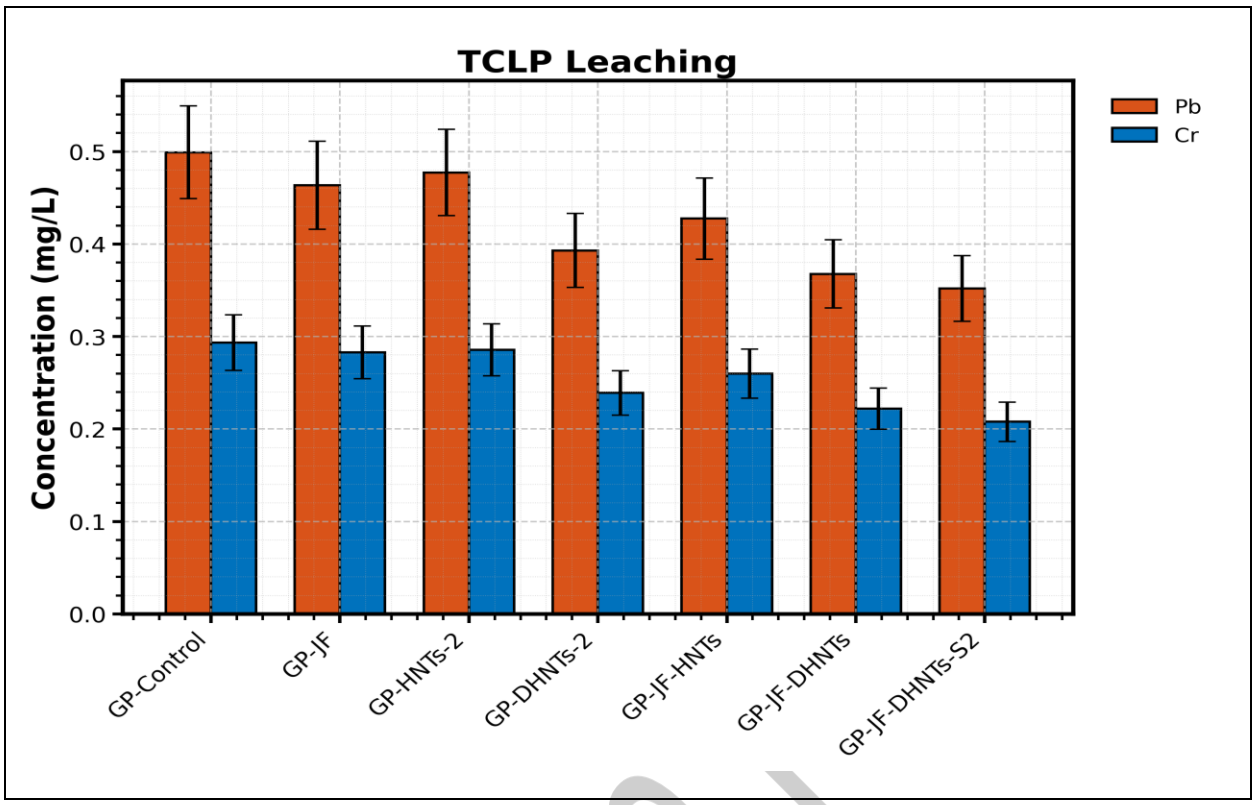

Fig. 16: TCLP leaching results showing heavy metal concentrations (Pb < 0.5 mg/L, Cr < 0.3 mg/L). D-HNTs composites exhibited slightly lower leaching values than the control, indicating that the precipitated carbonate phase enhances physical encapsulation and chemical stabilization, ensuring long-term safe confinement of immobilized species

3.8 Synergistic Mechanisms of CO_2 Capture and Immobilization

3.8.1 Role of Dopamine Functionalization

The experimental results firmly establish that dopamine functionalization is the critical enabler of the enhanced CO_2 capture performance. The chemisorption capacity of the material is directly derived from the polydopamine coating, which introduces abundant basic amine ($-NH_2$) groups onto the HNT surface. These amine groups act as specific capture sites for acidic CO_2 molecules. Through a Lewis acid-base interaction, the lone pair of electrons on the nitrogen atom of the amine group attacks the electrophilic carbon atom of the CO_2 molecule, forming a stable carbamate species. This chemical bond formation is significantly stronger than the weak van der Waals forces of physisorption, resulting in a substantial increase in both the total uptake capacity and the adsorption rate. Furthermore, the polydopamine layer serves a secondary, equally critical role: it acts as a nucleation promoter for mineralization. The catechol groups in polydopamine have a strong chelation affinity for calcium (Ca^{2+}) ions. By locally concentrating Ca^{2+} ions near the surface of the nanotubes, the polydopamine layer facilitates the immediate precipitation of $CaCO_3$ once CO_2 is chemisorbed, effectively converting the adsorbed gas into a stable mineral phase in situ (Feng *et al.* 2016; Zhao *et al.* 2007).

3.8.2 Role of Jute Fibers in Porosity Enhancement

The physical architecture of the composite is fundamentally altered by the inclusion of alkaline-treated jute fibers. While the D-HNTs provide the active chemical sites for adsorption and carbonation, the jute fibers provide the physical infrastructure required to maximize their utilization. The fibers create a well-connected network of macropores and interfacial pathways throughout the geopolymer matrix. This macroporous network effectively transforms the dense, monolithic binder into a highly porous, accessible framework. The significance of this structural modification lies in its effect on mass transport. Without these macropores, the bulk diffusion of CO_2 into the interior of the composite would be severely restricted by the high tortuosity of the mesoporous and microporous gel network. The interconnected channels provided by the fibers ensure that the CO_2 molecules can rapidly penetrate deep into the material, reaching the D-HNTs sites embedded within the bulk matrix, thereby overcoming mass-transfer limitations that typically hinder adsorption efficiency (Ahmed *et al.* 2025; Lo Bianco *et al.* 2024).

3.8.3 Hierarchical Pore Network Contribution

The combination of the micro-scale jute fibers and the nano-scale D-HNTs creates a meticulously engineered hierarchical pore network. Each length scale serves a distinct and complementary function, resulting in a highly optimized adsorption system. The macropores, which are primarily derived from the fiber-matrix interface, function as high-velocity, low-resistance transit routes for the bulk transport of CO_2 into the material. The mesopores, which are primarily contributed by the internal lumens of the HNTs and the nanoscale dispersion gaps, provide the high-specific-surface-area domains necessary for the chemisorption of CO_2 onto the amine functional groups. Finally, the microporosity intrinsic to the geopolymer gel itself acts as a final trapping stage, where any stray gas molecules can be confined. This multi-scale porosity eliminates the traditional adsorption bottleneck: a material can only adsorb gas as fast as it can deliver the gas to its binding sites. By providing separate pathways for rapid transport (macropores) and high-capacity binding (mesopores), the hierarchical network ensures both high rates of uptake and high equilibrium capacities (Chen *et al.* 2025; Li H *et al.* 2026).

3.8.4 Proposed Synergistic Mechanism

Based on the comprehensive data from the isotherm, kinetic, and mineralization studies, a robust, multi-step synergistic mechanism for the CO_2 capture and immobilization process is proposed. The process initiates with (i) Rapid Diffusion, where the CO_2 gas molecules are rapidly transported through the high-conductivity macropores provided by the jute fibers, bypassing potential diffusion bottlenecks. (ii) Chemisorption and Localization follows, where the gas molecules interact with the amine groups on the polydopamine layer of the D-HNTs, forming stable chemisorbed carbamate species. (iii) Ion Chelation and Precipitation occurs as the abundant Ca^{2+} ions released from the GGBFS are chelated by the polydopamine's catechol groups, creating a localized high-concentration zone that triggers the immediate precipitation of $CaCO_3$ around the nanotubes. Finally, (iv) Permanent Encapsulation is achieved as the surrounding geopolymer gel continues to polymerize and densify, physically enveloping the newly formed carbonate minerals within a rigid, highly stable aluminosilicate cage. This multi-step approach effectively transforms the captured CO_2 from a gaseous pollutant into a permanently safe mineral sink (Lo Bianco *et al.* 2024; Chaggar *et al.* 2025).

3.9 Comparative Performance with Literature

A comparative analysis of the synthesized geopolymer composite against recently reported CO_2 adsorbents and construction materials highlights the unique advantages of the proposed hierarchical design. Traditional geopolymer composites have been reported to achieve CO_2 adsorption capacities ranging from 0.2 to 0.5 mmol/g under similar temperature and pressure conditions, aligning with the baseline performance of the control formulation in this study. The incorporation of pristine nanomaterials, such as untreated carbon nanotubes or unmodified HNTs, typically offers a moderate improvement (increasing capacity to ~0.5–0.7 mmol/g), primarily acting through physical physisorption. The formulated GP-JF-DHNTs-S2 composite, which achieves a capacity exceeding 1.0 mmol/g, clearly outperforms these baseline materials, surpassing most geopolymer-based adsorbents reported in the literature (Pan *et al.* 2022; Chen *et al.* 2025). This performance is also competitive with advanced stabilized systems incorporating nano-silica and other nano-additives reported in recent studies (Vignesh et al. 2025a; Nanthini et al. 2024a). This superior performance can be attributed to the synergistic combination of chemisorption provided by the polydopamine coating and the enhanced mass transport enabled by the hierarchical pore network from the jute fibers. Furthermore, while many carbon-capturing adsorbents rely on complex, energy-intensive functionalization routes or expensive synthetic nanomaterials, the green, aqueous dopamine functionalization protocol and the use of naturally derived reinforcement (jute and HNTs) offer a significantly more sustainable and economically viable platform. Additionally, this composite moves beyond temporary reversible adsorption, offering a permanent, leak-proof mineral carbonation pathway for long-term carbon storage, which distinguishes it from reversible amine-grafted silicas that require frequent regeneration (Zhao *et al.* 2007; Chaggar *et al.* 2025).

3.10 Environmental and Economic Sustainability Assessment

The sustainability of the developed material system is derived from both its manufacturing methodology and its long-term functional goal. From an environmental perspective, the geopolymer binder replaces ordinary Portland cement (OPC), reducing the carbon footprint associated with construction materials by approximately 40-60%. The use of industrial by-products such as GGBFS and naturally occurring, abundant nanomaterials like halloysite further minimizes the reliance on energy-intensive synthetic additives. The dopamine functionalization process is performed in an aqueous, mildly alkaline (pH 8.5) Tris-HCl buffer, entirely eliminating the need for toxic organic solvents or harsh chemical reagents, thus adhering to the principles of green chemistry. The jute fibers are a renewable, biodegradable resource, adding a sustainable biomass component to the system. The long-term stability and environmental performance of such sustainable materials have been the focus of recent investigations, emphasizing the importance of durability assessment for infrastructure applications (Vilasini and Thangasamy 2025; Vilasini, 2026). Economically, the process utilizes standard, relatively inexpensive precursors and a simple aqueous

coating step, making the material highly scalable and cost-competitive compared to expensive synthetic polymer-based CO_2 adsorbents. Critically, the material does not just temporarily sequester CO_2; it permanently mineralizes it into a stable solid phase. This reduces the long-term economic burden of regeneration, maintenance, and potential leakage associated with traditional liquid amine scrubbing or reversible solid adsorbents. The composite therefore offers a dual benefit: it serves as a structural construction material while simultaneously acting as a permanent, non-hazardous carbon sink, contributing directly to circular economy principles and climate change mitigation goals (Pan *et al.* 2022; Chaggar *et al.* 2025).

4. CONCLUSIONS

This study successfully developed a multifunctional geopolymer composite by integrating a metakaolin-GGBFS binder with renewable jute fiber reinforcement and dopamine-functionalized halloysite nanotubes (D-HNTs). The aqueous dopamine functionalization protocol, conducted under mild alkaline conditions (pH 8.5) without toxic organic solvents, effectively introduced amine and catechol functional groups onto the HNT surface—confirmed by FTIR, XPS, and TEM analyses. The optimized hybrid composite, GP-JF-DHNTs-S2, achieved a 28-day compressive strength of 31.2 MPa and flexural strength of 5.7 MPa, with impact resistance enhanced by 68% over the control. These mechanical improvements are mechanistically attributed to the strong interfacial bonding between the polydopamine coating and the aluminosilicate gel network, combined with the crack-bridging function of the jute fibers.

The composite exhibited exceptional CO_2 uptake of 1.03 mmol/g at 25 °C and 1 atm—a 3.4-fold improvement over the control—with over 80% of equilibrium uptake achieved within 30 minutes. Adsorption kinetics followed a pseudo-second-order model ($R^2 > 0.99$), confirming that chemisorption on amine groups was the rate-limiting step. Critically, the captured CO_2 was not merely surface-adsorbed but actively converted into stable mineral phases. XRD (JCPDS No. 47-1743), FTIR, and XPS analyses confirmed calcite ($CaCO_3$) formation, with quantitative acid digestion revealing up to 7.0 wt% $CaCO_3$ precipitation. The material retained 85% of its initial adsorption capacity after 10 cycles, and TCLP tests confirmed the long-term stability of immobilized species.

The scientific contribution of this work lies in establishing a hierarchical adsorption-mineralization paradigm: jute fibers provide interconnected macropores for rapid gas transport, while polydopamine-coated HNTs deliver chemisorption sites and nucleation centers for $CaCO_3$ precipitation. This dual-functionality—structural reinforcement combined with permanent carbon sequestration—offers a transformative pathway for carbon-negative construction materials. Future work should focus on long-term durability under environmental weathering, pilot-scale implementation, and comprehensive life-cycle assessment to quantify the net carbon-negative potential.

FUNDING

This research received no specific grant from any funding agency in the public, commercial, or not-for-profit sectors.

CONFLICTS OF INTEREST

The authors declare that there is no conflict of interest.

REFERENCES

Abdullayev, E. and Lvov, Y., Halloysite for controllable loading and release, *Develop. Clay Sci.*, 7, 554-605 (2016). https://doi.org/10.1016/B978-0-08-100293-3.00022-4

Ahmed, J. P. S., Kaviyan, M., Sivakumar, Y. and Shanmugavel, S., Exploring the role of halloysite nanotubes in improving carbon fiber reinforced composite performance across diverse temperatures, *Eng. Res. Exp.*, 7(4), 045521 (2025). https://doi.org/10.1088/2631-8695/ae0f04

Al-Naghi, A. A., Ghazouani, N. and Elhadi, K. M., Thermo-Carbonation synergy for enhanced CO_2 sequestration and performance of activated bauxite residue-based geopolymer composites, *J. Sustain. Cem.-Based Mater.*, 1-23 (2026). https://doi.org/10.1080/21650373.2026.2696353

Andrew, R. M., Global CO_2 emissions from cement production, 1928–2018, *Earth Syst. Sci. Data*, 11(4), 1675-1710 (2019). https://doi.org/10.5194/essd-11-1675-2019

Bakri, O. M. and Mahmoud, A. A., CO_2-Binder Reaction Mechanisms in Geopolymer Wellbore Cements: Alternatives to API Class G Cement in CO_2-Rich Environments (CCS), *Mol.*, 31(4), 620 (2026). https://doi.org/10.3390/molecules31040620

Bernal, S. A., Microstructural changes induced by CO_2 exposure in alkali-activated slag/metakaolin

pastes, *Front. Mater.*, 3, 43 (2016). https://doi.org/10.3389/fmats.2016.00043

Çevik, A. and Niş, A., Introduction to fiber-reinforced alkali-activated composites, *Adv. Fib. Reinforce. Alkali-Activated Compos.*, 1-21 (2023). https://doi.org/10.1016/B978-0-443-15301-3.00007-5

Chaggar, P. K., Javan, K., Duarte, M. C., Darestani, M. and Markhali, B. P., Dynamic CO_2 sequestration: from global emission challenges to sustainable capture through geopolymer technologies, *Environ. Sci. Pollut. Res.*, 32(46), 26068-26087 (2025). https://doi.org/10.1007/s11356-025-37222-5

Chen, H., Yang, Y., Wei, W., Cavallaro, G., Zhai, Z., Zhao, Y., Wang, D., Chen, S., Shang, H. and Zhang, B., Superhydrophobic halloysite-based porous foamed geopolymer for efficient phase change material encapsulation with enhanced thermal management performance, *Appl. Clay Sci.*, 284, 108133 (2026). https://doi.org/10.1016/j.clay.2026.108133

Chen, Q., Chen, Y., Kang, J. and Chen, F., Carbonation impact on the stabilization of heavy metals in carbon-rich geopolymers based on gasification slag and fly ash, *Environ. Pollut.*, 382, 126671 (2025). https://doi.org/10.1016/j.envpol.2025.126671

da Rocha Loures, F. S., Sichonany, A. V., Mortari, S. R., Floss, M. F., da Silva, W. L. and da Silva, C. L., Aplicação de nanotubos de carbono em concreto: uma revisão técnica, *Disciplinarum Scientia | Naturais e Tecnológicas*, 27(2), 61-85 (2026). https://doi.org/10.37779/nt.v27i2.5615

Das, S. C., Das, S. C., Rahman, M. M., Sayeed, M. A., Khan, M. M., Jahan, M. S. and Islam, T., Analysis of mechanical and thermal properties of hybrid FRP composites with short jute, coir and glass fibers—effects of different fiber loading and waste valorization, *Mater. Circ. Econ.*, 7(1), 42 (2025). https://doi.org/10.1007/s42824-025-00197-2

Davidovits, J., Geopolymers based on natural and synthetic metakaolin: a critical review, *Proce. 41st Int. Conf. Adv. Ceram. Compos. Ceram. Eng. Sci. Proce.*, 38(3), 38(2018). https://doi.org/10.1002/9781119474746.ch19

Fan, L., Xu, F., Wang, S., Yu, Y., Li, P., Zhang, J. and Yu, L., Role of halloysite nanotubes in modulating the mechanical and microstructural characteristics of geopolymer concrete under thermal curing, *Constr. Build. Mater.*, 472, 140897 (2025). https://doi.org/10.1016/j.conbuildmat.2025.140897

Feng, J., Fan, H., Zha, D. A., Wang, L. and Jin, Z., Characterizations of the formation of polydopamine-coated halloysite nanotubes in various pH environments, *Langmuir*, 32(40), 10377-10386 (2016). https://doi.org/10.1021/acs.langmuir.6b02948

Hassan, H. S., Shi, C., Hashem, F. S., El-Magd, S. A., Maged, A., Abdel-Gawwad, H. A. and Pfeiffer, H., Industrial waste recycling approach: An ecofriendly geopolymer binder for clean and sustainable environments (A 24-h green recycling process), *J. Environ. Manage.*, 377, 124568 (2025). https://doi.org/10.1016/j.jenvman.2025.124568

Islam, S., Karim, F. E. and Islam, M. R., Assessing the consequences of water retention on the structural integrity of jute fiber and its composites: a review, *SPE Polym.*, 5(4), 457-480 (2024). https://doi.org/10.1002/pls2.10142

Jagajeevan, V. and Sivakumar, V. L., Environmental fate mapping of lead-free piezoelectrics: Synergistic stress-induced leaching kinetics and multi-trophic dose-response in BFO/rGO hybrids, *Chemosphere*, 409, 145001 (2026). https://doi.org/10.1016/j.chemosphere.2026.145001

Joussein, E., Petit, S., Churchman, J., Theng, B., Righi, D. and Delvaux, B. J., Halloysite clay minerals—a review, *Clay Miner.*, 40(4), 383-426 (2005). https://doi.org/10.1180/0009855054040180

Kavitha, S. S., Sarker, P. K., Madhavan, M. K. and Jayanarayanan, K., Sustainable approach for the confinement of concrete cylinders using fiber-reinforced polymers with bio-based hemp and halloysite nano tubes, *Polym. Compos.*, 47(12), 11377-11393 (2026). https://doi.org/10.1002/pc.71028

Li, B., Ma, J., Long, K., Zhang, J., Gao, Y. and Liu, H., CO_2 mineralization with fly ash for underground carbon-negative backfill: Carbon sequestration and heavy metal immobilization, *J. CO_2 Util.*, 106, 103366 (2026). https://doi.org/10.1016/j.jcou.2026.103366

Li, H., Gao, L., Huang, L. and Li, Y., A comprehensive environmental impact evaluation of underground wastewater treatment plant: Integrating greenhouse gas emissions, environment footprint, and economic assessments, *Process Saf. Environ. Prot.*, 211, 108748 (2026). https://doi.org/10.1016/j.psep.2026.108748

Lo Bianco, A., Calvino, M. M., Cavallaro, G., Lisuzzo, L., Pasbakhsh, P., Milioto, S., Lazzara, G. and Lvov, Y., Flame-resistant inorganic films by self-assembly of clay nanotubes and their conversion to geopolymer for CO_2 capture, *Small*, 20(51), 2406812 (2024). https://doi.org/10.1002/smll.202406812

Mastali, M., Kinnunen, P., Isomoisio, H., Karhu, M. and Illikainen, M., Mechanical and acoustic properties of fiber-reinforced alkali-activated slag foam concretes containing lightweight structural aggregates, *Constr. Build. Mater.*, 187, 371-381 (2018). https://doi.org/10.1016/j.conbuildmat.2018.07.228

Murmu, A. L., Dhole, N. and Patel, A., Stabilisation of black cotton soil for subgrade application using fly ash geopolymer, *Road Mater. Pavement Des.*, 21(3), 867-885 (2020). https://doi.org/10.1080/14680629.2018.1530131

Nanthini, M., Ganesan, R. and Jaganathan, V., Incorporation of nanoalumina in potassium feldspar-based phosphoric acid activated geopolymer composites: a sustainable approach, *J. Environ. Nanotechnol.*, 13(3), 89-98 (2024). https://doi.org/10.13074/jent.2024.09.243840

Nanthini, M., Ganesan, R. and Jaganathan, V., Experimental Investigation of the Durability of Ambient-Cured Metakaolin-Based Geopolymer Concrete in Different Sustainable Environmental Conditions, J. Environ. Nanotechnol., 13(3), 73-81 (2024). https://doi.org/10.13074/jent.2024.09.242754

Pan, Z., Zhang, C., Li, Y. and Yang, C., Solidification/stabilization of gold ore tailings powder using sustainable waste-based composite geopolymer, *Eng. Geol.*, 309, 106793 (2022). https://doi.org/10.1016/j.enggeo.2022.106793

Praveenkumar, S., Vishvanathperumal, S., Ramu, K. N. and Manimaran, K., Influence of halloysite nanotubes (HNTs) and their TESPT-, APTES-, and GPTMS-modified forms on the curing, mechanical, and swelling behavior of SBR/NBR composites, *J. Mater. Eng. Perform.*, 35, 27157-27172(2026). https://doi.org/10.1007/s11665-026-13530-w

Provis, J. L., Palomo, A. and Shi, C., Advances in understanding alkali-activated materials, *Cem. Concr. Res.*, 78, 110-125 (2015). https://doi.org/10.1016/j.cemconres.2015.04.013

Reddy, A. S., Iyer, K. K., Rotte, V. M. and Dave, T. N., Performance of alkali activated slag stabilized landfill mined soil-like fraction exposed to different climatic conditions, *Int. J. Geosynth. Ground Eng.*, 10(5), 80 (2024). https://doi.org/10.1007/s40891-024-00593-9

Shi, J., Shen, Y., Zhang, W., Fu, Y. and Kong, X., Effects of three different nanomaterials on the properties and microstructure of sludge based geopolymers, *Constr. Build. Mater.*, 414, 134965 (2024). https://doi.org/10.1016/j.conbuildmat.2024.134965

Singh, R. and Budarayavalasa, S., Solidification and stabilization of hazardous wastes using geopolymers as sustainable binders, *J. Mater. Cycles Waste Manage.*, 23(5), 1699-1725 (2021). https://doi.org/10.1007/s10163-021-01245-0

Srinivasan, K., Vivek, S. and Sampathkumar, V., Facilitating Eco-Friendly Construction Practices with the Sustainable Application of Nanomaterials in Concrete Composites, J. Environ. Nanotechnol., 13(2), 201-207 (2024). https://doi.org/10.13074/jent.2024.06.242556

Thomas, J., Thomas, P. S. and Stephen, R., Improved mechanical, thermal, and barrier properties of halloysite nanotubes and nanocellulose incorporated PVA-PEO films: For food packaging applications, *Food Packag. Shelf Life*, 46, 101373 (2024). https://doi.org/10.1016/j.fpsl.2024.101373

Vignesh, J., Sivakumar, V. L., Kandasamy, A. and Al Khazaleh, M., Green engineering of surfactant-assisted nano silica dispersion in alkaline cementitious systems using chitosan, *J. Environ. Nanotechnol.*, 14(3), 750-765 (2025). https://doi.org/10.13074/jent.2025.09.2531777

Vignesh, J., Sivakumar, V. L., Kandasamy, A. and Al Khazaleh, M., Bio-derived kraft lignin as a green stabilizer for surfactant-assisted nano silica dispersion in cementitious systems, *J. Environ. Nanotechnol.*, 14(3), 766-780 (2025). https://doi.org/10.13074/jent.2025.09.2531781

Vilasini, P. P. and Thangasamy, L., Comparative long-term stabilization of pond ash using lime and cement: FTIR characterization, strength optimization and sustainable utilization, *Next Mater.*, 8, 100908 (2025). https://doi.org/10.1016/j.nxmate.2025.100908

Vilasini, P. P., Integrated mechanical, durability and environmental assessment of stabilized pond ash, *Next Mater.*, 13, 102769 (2026). https://doi.org/10.1016/j.nxmate.2026.102769

Walbrück, K., Maeting, F., Witzleben, S. and Stephan, D., Natural fiber-stabilized geopolymer foams—A review, *Mater.*, 13(14), 3198 (2020). https://doi.org/10.3390/ma13143198

Wang, P., Shi, M., Shu, Y., Niu, Q. and Zhang, P., Porous $CaCO_3$ fabricated by Ca-containing solid wastes for effective CO_2 adsorption, *J. Environ. Chem. Eng.*, 13(2), 115815 (2025). https://doi.org/10.1016/j.jece.2025.115815

Wang, Y., Liu, L., Ren, C., Ma, J., Shen, B., Zhao, P. and Zhang, Z., A novel amine functionalized porous geopolymer spheres from municipal solid waste incineration fly ash for CO_2 capture, *J. Environ. Manage.*, 349, 119540 (2024). https://doi.org/10.1016/j.jenvman.2023.119540

Xu, J., Kang, A., Wu, Z., Gong, Y. and Xiao, P., The effect of mechanical-thermal synergistic activation on the mechanical properties and microstructure of recycled powder geopolymer, *J. Cleaner Prod.*, 327, 129477 (2021). https://doi.org/10.1016/j.jclepro.2021.129477

Zhao, H., Hu, J., Wang, J., Zhou, L. and Liu, H., CO_2 capture by the amine-modified mesoporous materials, *Acta Phys.-Chim. Sin.*, 23(6), 801-806 (2007). https://doi.org/10.1016/S1872-1508(07)60046-1